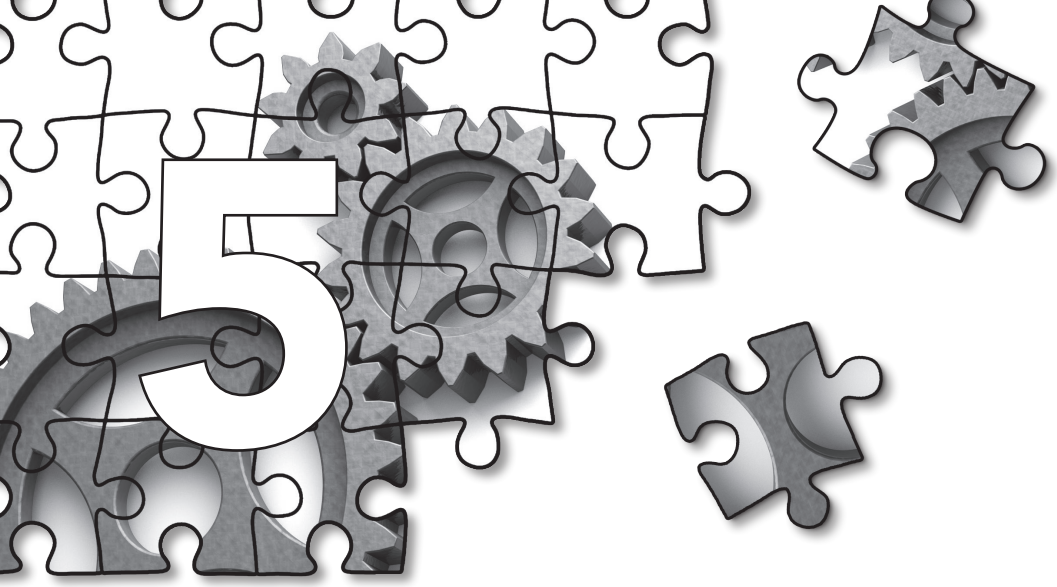

VACCINATION DURING MYELOID CELL DEPLETION BY CANCER CHEMOTHERAPY FOSTERS ROBUST T-CELL RESPONSES

Marij J. Welters*, Tetje C. van der Sluis*, Hélène van Meir*, Nikki M. Loof, Vanessa J. van Ham, Suzanne van Duikeren, Saskia J Santegoets, Ramon Arens, Marieke L. de Kam, Adam F. Cohen, Mariette I. van Poelgeest, Gemma G. Kenter, Judith R. Kroep, Jacobus Burggraaf, Cornelis J. Melief, Sjoerd H. van der Burg

* Authors contributed equally to the study and share first authorship

Science Translational Medicine, 2016;8:334ra52.

ABSTRACT

Therapeutic vaccination with human papillomavirus type 16 synthetic long peptides (HPV16-SLPs) results in T cell–mediated regression of HPV16-induced premalignant lesions but fails to install clinically effective immunity in patients with HPV16-positive cervical cancer. We explored whether HPV16-SLP vaccination can be combined with standard carboplatin and paclitaxel chemotherapy to improve immunity and which time point would be optimal for vaccination. This was studied in the HPV16 E6/E7–positive TC-1 mouse tumor model and in patients with advanced cervical cancer. In mice and patients, the presence of a progressing tumor was associated with abnormal frequencies of circulating myeloid cells. Treatment of TC-1–bearing mice with chemotherapy and therapeutic vaccination resulted in superior survival and was directly related to a chemotherapy-mediated altered composition of the myeloid cell population in the blood and tumor. Chemotherapy had no effect on tumor-specific T cell responses. In advanced cervical cancer patients, carboplatin-paclitaxel also normalized the abnormal numbers of circulating myeloid cells, and this was associated with increased T cell reactivity to recall antigens. The effect was most pronounced starting 2 weeks after the second cycle of chemotherapy, providing an optimal immunological window for vaccination. This was validated with a single dose of HPV16-SLP vaccine given in this time window. The resulting proliferative HPV16-specific T cell responses were unusually strong and were retained after all cycles of chemotherapy. In conclusion, carboplatin-paclitaxel therapy fosters vigorous vaccine-induced T cell responses when vaccination is given after chemotherapy and has reset the tumor-induced abnormal myeloid cell composition to normal values.

INTRODUCTION

Most cervical cancers are induced by human papillomavirus type 16 (HPV16) (1). Up to 70% of the advanced cancers relapse (2, 3). One of the preferred treatments for patients with recurrent, metastatic, or advanced cervical carcinoma is the combination of carboplatin with paclitaxel (CarboTaxol) (4), but this is rarely curative (5).

The two HPV16-encoded oncoproteins E6 and E7 are required for the transformation of epithelial cells (6) and constitute excellent targets for the immune system. HPV16-specific T cell reactivity is frequently detected in healthy individuals but usually not in patients with premalignant anogenital lesions or cancer (7). Installment of robust HPV16-specific immunity by vaccination with therapeutic HPV16 overlapping synthetic long peptides (HPV16-SLPs) admixed with Montanide ISA-51 resulted in regressions of HPV16-induced premalignant lesions of the vulva in two independent studies (8-10). In contrast, therapeutic vaccination of patients with advanced or recurrent HPV16-positive cervical cancer partly installed HPV16-specific T cell reactivity, particularly in patients with a less suppressed immune status, but had no clinical effect (11).

Chemotherapeutic agents act on cancer cells (12), but many of them mediate part of their therapeutic effects through immune mechanisms (13, 14). In murine models, the combination of chemotherapy with activation of T cells resulted in improved treatment of tumors (13-16). Therefore, we investigated whether CarboTaxol could be successfully combined with HPV16-SLP vaccination, first in a mouse model and then in an open-label observational study with cervical cancer patients.

MATERIALS AND METHODS

Study design

The aim of the study was to test whether CarboTaxol could be combined with HPV16-SLP vaccination. We first used the HPV16 E6/E7–expressing TC-1 tumor mouse model to define the impact of CarboTaxol on systemic and intratumoral immunological parameters as well as on the clinical efficacy of vaccination. After observing that CarboTaxol did not affect lymphocytes but had a strong effect on myeloid cells and improved tumor control by therapeutic vaccination, we started a multicenter, open-label, observational study, entitled "Immunological aspects of combined chemo-immunotherapy in patients with advanced cervical cancer" (EudraCT 2010-018841-76), consisting of two cohorts of patients. In the first cohort, six patients with advanced, recurrent, or metastatic cancer were treated with six cycles of CarboTaxol every 3 weeks, and the composition and function of the myeloid and lymphoid cells in peripheral blood were analyzed. After identifying a specific time window during chemotherapy potentially permitting the best T cell response, we studied the second cohort of patients. In this cohort, 12 patients were treated with CarboTaxol and one dose of an HPV16-SLP vaccine 2 weeks after the second cycle of CarboTaxol. Blood samples were drawn to validate the observations made in the first cohort as well as to study the vaccine-induced T cell response. The investigators performing and analyzing immunological assays were blinded to the clinical parameters of the patients. The data from the immunomonitoring studies are reported according to the recommended standard format "minimal information about T cell assays."

Mice and tumor treatment

Female C57BL/6 mice (6 to 8 weeks old; Charles River Laboratories) were housed in individually ventilated cage systems under specific pathogen–free conditions. The experiments were approved by the Animal Experiments Committee of Leiden University Medical Center (LUMC), in line with the guidelines of the European Committee.

The tumor cell line TC-1 is of C57BL/6 origin and expresses HPV16 E6 and E7 (17). TC-1 tested negative for rodent viruses by polymerase chain reaction. Mice were subcutaneously inoculated with 1×10^5 TC-1 tumor cells. When a palpable tumor was present on day 8, mice were split into groups with comparable tumor size and treated with carboplatin [40 mg/kg, day 8, intraperitoneally], paclitaxel (20 mg/kg, days 8 and 9, intraperitoneally), and/or subcutaneous synthetic long HPV16 $E7_{43–77}$ peptide (SLP; GQAEPDRAHYNIVTFCCKCDSTLRLCVQSTHVDIR; 150 μg) dissolved in dimethyl sulfoxide (Sigma), diluted in phosphate-buffered saline (B. Braun), and emulsified in Montanide ISA-51 (Seppic). Chemotherapy was repeated 1 week later (day 15 for carboplatin and days 15 and 16 for paclitaxel), and vaccination was repeated 2 weeks after initial treatment (day 22). Detailed information on the immunomonitoring and statistics is given in the Supplementary Materials.

PATIENTS

Patients with clinical and radiological evidence of advanced-stage, recurrent, or metastatic cervical cancer; with no curative treatment options; and scheduled for CarboTaxol were enrolled between January 2011 and January 2013. Other inclusion criteria were as follows: (i) mentally competent patients 18 years or older, (ii) no other active malignancy, (iii) no indication of active infectious disease such as HIV, (iv) and no other condition that may jeopardize the health status of the patient. Patients were followed until 2 to 3 weeks after they had received their last chemotherapy cycle and thereafter at standard visits. LUMC, Academic Medical Center (Amsterdam), Free University Medical Center (Amsterdam), and Netherlands Cancer Institute–Antoni van Leeuwenhoek Hospital (Amsterdam) were the participating hospitals.

HPV typing was performed on the tumor and/or smears taken at study entry (8), but it was not part of the inclusion criteria. The study was conducted in accordance with the Declaration of Helsinki (October 2008) and approved by the Central Committee on Research Involving Human Subjects (NL31572.000.10) in agreement with the Dutch law for medical research involving humans.

Treatment of patients

For the first cohort, six of the nine screened and eligible patients participated and were treated at their hospital with CarboTaxol, consisting of carboplatin (dose based on renal function; area under the curve of six regimen) and paclitaxel (175 mg/kg^2) on day 1 of each cycle, every 3 weeks for a maximum of six cycles. The patients were subjected to serial blood sampling. According to the oncology protocols, routine premedication consisting of dexamethasone [20 mg, intravenously (iv)], ranitidine (50 mg in 100 ml of NaCl 0.9%, iv), granisetron (1 mg in 100 ml of NaCl 0.9%, iv), and clemastine (2 mg in 100 ml of NaCl 0.9%, iv) was administered immediately before chemotherapeutic treatment. In case of severe hematological toxicity,

neurotoxicity, nephrotoxicity, or gastrointestinal toxicity, dose modifications of carboplatin and paclitaxel were made according to the following standard scheme: (i) if the absolute neutrophil count was $<1.5 \times 10^9$/liter, platelet count was $<100 \times 10^9$/liter, or other toxicities were higher than grade 2, then CarboTaxol treatment was postponed for at least a week (or longer until the patients had recovered), and the doses of both chemotherapeutic compounds were reduced by 25%; (ii) if the patient experienced neuropathy higher than grade 2, paclitaxel was stopped but carboplatin was continued. After the completion of immunomonitoring of these first 6 patients, a second group of 12 patients (cohort 2) received CarboTaxol at their hospital at the same schedule and dose, as well as a single subcutaneous vaccination of the HPV16-SLP vaccine (300 μg per peptide emulsified in Montanide ISA-51) consisting of two mixes of peptides injected separately in the left and right limb (either arm or leg) (9) at LUMC, 2 weeks after the second cycle of CarboTaxol. For cohort 2, 18 advanced cervical cancer patients were screened, 5 patients declined participation, and 1 patient (ID6002) died of her disease before receiving the vaccine.

Clinical evaluation of safety and tolerability

The safety and toxicity of treatment were evaluated according to the National Cancer Institute CTCAE v3.0. Well-known toxicities of CarboTaxol were classified as study-related events. Before the start of CarboTaxol and before vaccination, patients were physically examined and medical history was obtained. Vital signs were measured, and the injection site was inspected 15 min, 1 hour, and 4 hours after vaccination. Patients were followed with routine visits (every 3 months until progression) to monitor for AEs. For each vaccine-related AE, the relationship to HPV16-SLP was defined as definite, probable, or possible. Injection site reactions were classified as definitely vaccine-related. Injection site reaction grade 1 was defined as swelling, erythema, and tenderness (pain/itching). Injection site reaction grade 2 was defined as tenderness or swelling with inflammation or phlebitis. Injection site reaction grade 3 was defined as severe ulceration or necrosis. Venous blood samples were drawn for routine hematological analysis, including leukocyte differential counts and biochemistry assessments. Patients were followed up until date of death or loss to follow-up.

Immunomonitoring of clinical trial

Blood samples from patients were taken at the time points indicated in Fig. 4A. In addition, 19 healthy volunteers donated blood. PBMCs were isolated by Ficoll gradient centrifugation, and cells were subjected to LST (9-11). MRM and influenza peptide pools served as positive controls. The remaining cells were cryopreserved until use. Thawed PBMCs were tested for their response to PHA in a proliferation assay (18, 19), for their antigen-presenting capacity in an MLR (19), and for their HPV16-specific T cell responses by intracellular cytokine staining (10). The 11-day stimulated nondepleted and CD14-depleted PBMC samples were analyzed by a proliferation assay for antigen recognition (20). The supernatants of the proliferation assays were used for cytokine analysis by cytometric bead array (9-11). Immunophenotyping of the PBMC samples was performed by flow cytometry (19). Detailed information on immunomonitoring and statistics is given in the Supplementary Materials.

RESULTS

Combined chemoimmunotherapy improves the eradication of HPV16-positive tumors in mice

To test the effects of CarboTaxol with HPV16-SLP vaccination, HPV16 E6– and E7–positive TC-1 tumor-bearing mice were treated when tumors were palpable at day 8 (~4 mm^2; Fig. 1A). CarboTaxol had little effect on tumor growth, whereas vaccination induced a temporary decrease in tumor size (Fig. 1, B and C). The combined treatment had the strongest antitumor effect (Fig. 1, B and C). None of the treatments affected the percentages of circulating $CD8^+$ and $CD4^+$ T cells (Fig. 1, D and E, and fig. S1, A and B). Vaccination induced HPV16-specific $CD8^+$ T cells, and this was not influenced by co-treatment with CarboTaxol (Fig. 1F and fig. S1C).

CarboTaxol treatment alters circulating and intratumoral myeloid cell populations

To understand the mechanism underlying these improved therapeutic outcomes, immune cells in blood and tumors were analyzed 3 to 4 days after CarboTaxol treatment (and/or 9 to 10 days after peptide vaccination) (Fig. 2A), which is at the start of the tumor regression phase (fig. S2). In untreated tumor-bearing mice, the percentage of circulating myeloid cells increased (fig. S3A) because of the increase in circulating $CD11b^{hi}$ cells, in particular, $CD11b^{hi}Gr\text{-}1^{hi}$ cells. However, their numbers decreased markedly in tumor-bearing animals treated with CarboTaxol (Fig. 2, B and C, and fig. S3). The frequencies of $CD4^+$ and $CD8^+$ T cells, antigen-specific $CD8^+$ T cells, monocytes, and dendritic cells in the blood were not affected by CarboTaxol treatment (fig. S3). Thus, CarboTaxol treatment normalized the myeloid cell populations in the blood of tumor-bearing mice, making them more similar to those of naïve mice. This effect could not be ascribed to one individual chemotherapeutic compound because the effect on circulating $CD11b^{hi}$ cells was particularly pronounced in animals treated with both compounds (fig. S4).

Next, we assessed the effects of CarboTaxol-vaccine combination treatment on the tumor microenvironment. The percentage of intratumoral leukocytes increased upon treatment with CarboTaxol and/or vaccine (Fig. 2D). In vaccinated mice, a markedly high percentage of these leukocytes were $CD8^+$ T cells (Fig. 2E), half of which were vaccine-specific (Fig. 2F) and capable of producing IFN-γ and TNFα (Fig. 2G). There was no direct effect of CarboTaxol treatment on the presence and function of these lymphocytes.

We then focused on the intratumoral $CD11b^{hi}$ myeloid cells because the $Gr\text{-}1^{hi}$ subtype of this cell population was increased in the blood of untreated tumor-bearing mice. The $Gr\text{-}1^{hi}$ cells in the tumors strongly expressed the granulocytic marker Ly6G and decreased amounts of the macrophage marker F4/80 and the dendritic cell marker CD11c. In contrast, $Gr\text{-}1^{int}$ cells had a higher expression of F4/80, CD11c, CD80, CD86, and major histocompatibility complex class II, but not Ly6G (Fig. 3A), suggesting a superior immune stimulatory capacity. Treatment with either CarboTaxol or vaccine resulted in a predominance of the $CD11b^{hi}Gr\text{-}1^{int}$ population over the $Gr\text{-}1^{hi}$ population (Fig. 3, B and C). Together, these data demonstrate that treatment of tumor-bearing mice with CarboTaxol results in a relative loss of myeloid cell–associated immunosuppression in both tumor and blood.

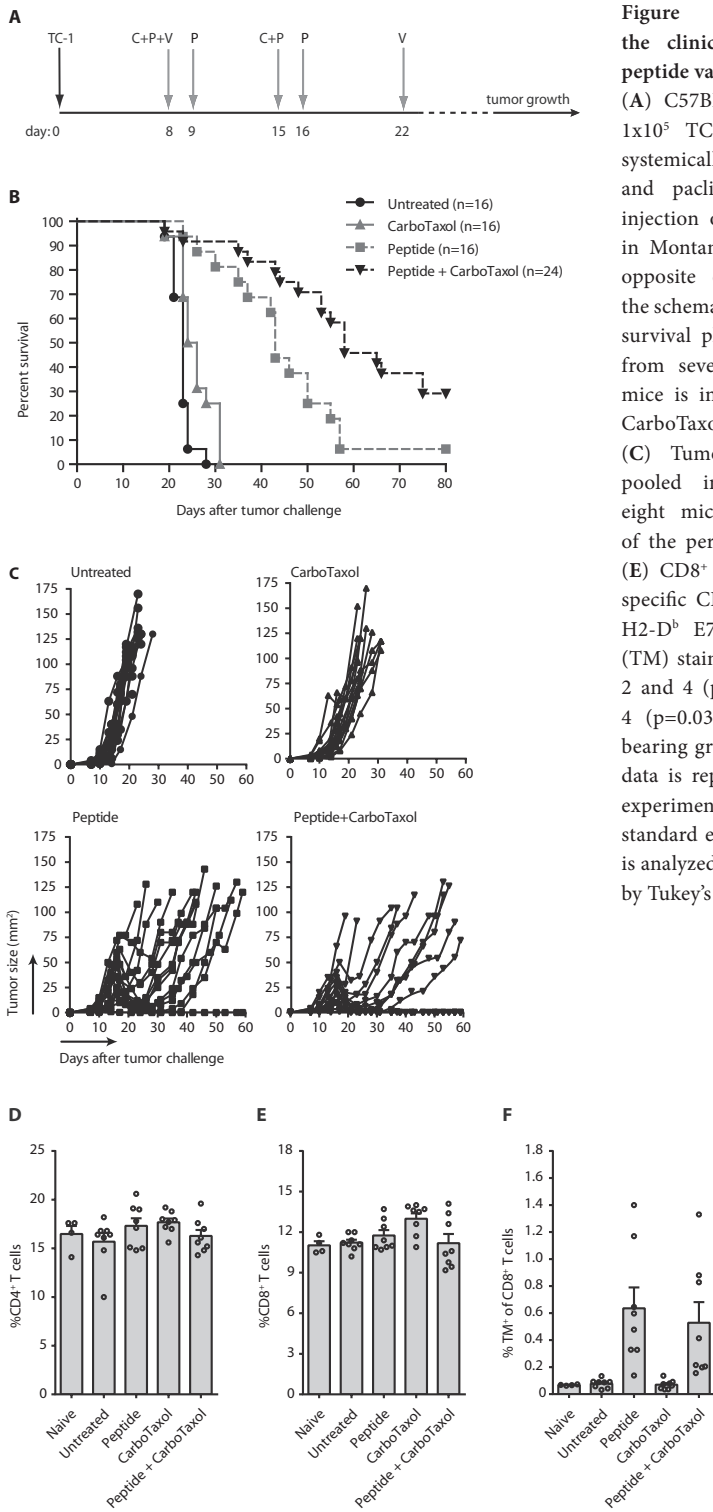

Figure 1. CarboTaxol improves the clinical outcome of therapeutic peptide vaccination.
(**A**) C57BL/6 mice were injected with $1x10^5$ TC-1 tumor cells and treated systemically with carboplatin (C) and paclitaxel (P) with or without injection of the HPV16 $E7_{43-77}$ peptide in Montanide vaccine (V) in the flank opposite of the tumor according to the schematic diagram. (**B**) Kaplan-Meier survival plots show the combined data from several experiments (number of mice is indicated). Peptide *vs* peptide-CarboTaxol treated group (p=0.004). (**C**) Tumor growth data from two pooled individual experiments with eight mice per group. Quantification of the percentage of (**D**) $CD4^+$ T cells, (**E**) $CD8^+$ T cells and (**F**) the vaccine-specific $CD8^+$ T cells as determined by H2-D^b $E7_{49-57}$ (RAHYNIVTF) tetramer (TM) staining. Column 3 *vs* 1 (p=0.03), 2 and 4 (p=0.005). Column 5 *vs* 2 and 4 (p=0.03). N=8 mice in the tumor-bearing groups, N=4 in the naïve group, data is representative of two individual experiments and expressed as mean plus standard error of the mean (SEM). Data is analyzed by one-way ANOVA followed by Tukey's post-hoc analysis.

A specific time window is associated with increased immunity in patients on chemotherapy

On the basis of the above observations, we performed a study in patients with advanced, recurrent, or metastatic cervical carcinoma. The trial was designed to study the impact of chemotherapy on vaccine-induced immunity, and therefore patients were not required to have an HPV16$^+$ tumor. Patients were screened between January 2011 and January 2013 in four Dutch hospitals, and their characteristics are listed in table S1. In the first cohort of six patients, the number and function of lymphoid and myeloid cells were studied in blood samples taken at different time points during and after CarboTaxol treatment (Fig. 4A). CarboTaxol treatment was associated with a decrease in the otherwise high frequency of myeloid cells (median of 32% at baseline), which reached its nadir at 1 to 2 weeks after the second chemotherapy cycle (median of 6% at 1 to 2 weeks after chemotherapy cycle 2; Fig. 4, B and C) and coincided with an increase in the percentages of lymphoid cells (Fig. 4D). Although the relative frequencies of CD4$^+$ and CD8$^+$ T cells (fig. S5) remained unchanged, T cell function was improved, as evidenced by the increase in their proliferation against a bacterial recall antigen mixture [memory response mix (MRM)] in the same time window (Fig. 4E). T cell responses to phytohemagglutinin (PHA) stimulation were strong at all time points, indicating that there were no intrinsic problems with the T cells' response to mitogens (fig. S5). The capacity of antigen-presenting cells (APCs) to stimulate allogeneic T cell proliferation was slightly improved (Fig. 4F). Thus, the observations in mice are mirrored by the findings in patients. Furthermore, the results revealed a specific time window throughout CarboTaxol treatment, during which antigen-specific T cell responses were optimal. This time window, starting at 1 to 2 weeks after the second cycle of CarboTaxol, appeared attractive for the generation of strong T cell responses by vaccination. We used this observation to select the time window for the application of a single dose of vaccine in the second patient cohort.

CarboTaxol mediates normalization of circulating immune cell frequencies

The second cohort consisted of 13 patients (table S1). One patient (ID6002) died of progressive disease before vaccination and was substituted by ID6102. Compared to 19 healthy donors, the patients from both cohorts displayed an increased frequency of circulating myeloid cells before chemotherapy (fig. S6A), confirming that the progressive tumor growth–induced myeloid changes in mice are mirrored in patients with advanced cervical cancer (Fig. 4). Throughout the CarboTaxol treatment, the absolute numbers of lymphocytes remained similar (Fig. 5A), but the absolute number of circulating leukocytes was strongly reduced (median, -4.7×10^9/liter) as measured by leukocyte differentiation analyses (Fig. 5B). This reduction reached its nadir after two cycles of chemotherapy and was retained during the remainder of the chemotherapy cycles. Flow cytometry analysis again revealed a decrease in myeloid (CD45$^+$CD3$^-$CD19$^-$) and a relative increase in lymphoid (CD45$^+$CD3$^+$CD19$^-$) cells (fig. S6, B and C). The frequency of these populations almost normalized to the levels observed in healthy donors (Fig. 5, C and D), and this correlated with an increased T cell responsiveness to bacterial (MRM; Fig. 5E) and viral antigens (FLU; Fig. 5F). Similar to the first cohort, the blood samples of cohort 2 showed no overt changes in APC function or the response to PHA stimulation (fig. S5).

Further dissection of the changes within the myeloid ($CD45^+CD3^-CD19^-CD1a^-$) cell population was performed on the basis of HLA-DR (human leukocyte antigen–DR) expression to distinguish macrophages and dendritic cells ($HLA\text{-}DR^+$) from myeloid-derived suppressor cells (MDSCs; $HLA\text{-}DR^{-/low}$) and further subdivide them on the expression of CD14 and CD11b within the $HLA\text{-}DR^+$ myeloid cell population (fig. S7). Of the five identified subpopulations, population 1 ($CD14^+CD11b^+$) and population 2 ($CD14^{int}CD11b^{int}$) were most abundant and increased before CarboTaxol treatment when compared to healthy donors (Fig. 6, A and B, and fig. S8). The other three populations each constituted 0.2 to 2.6% of the myeloid cell fraction. During chemotherapy, the frequencies of populations 1, 3, and 5 dropped (Fig. 6B and fig. S8). The treatment-induced decrease in population 1 coincided with improved T cell reactivity against MRM and FLU (Fig. 6C). Extended analysis of the various subsets by flow cytometry (fig. S7) revealed that population 1 was composed of M1 monocytes/macrophages ($CD45^+CD3^-CD19^-CD1a^-HLA\text{-}DR^+CD14^+CD11b^+CD206^-CD163^-CD16^-CD11c^+$) and M2c monocytes/macrophages ($CD45^+CD3^-CD19^-CD1a^-HLA\text{-}DR^+CD14^+CD11b^+CD206^-CD163^+CD16^-CD11c^+$). The frequency of both subpopulations was increased in patients but normalized upon treatment (Fig. 6, D and E). The frequency of 10 distinct circulating MDSC populations (21) was not different between patients and healthy donors. Only the main MDSC population ($CD45^+CD3^-CD19^-CD1a^-HLA\text{-}DR^{low}$) displayed a slight decrease during chemotherapy (Fig. 6F and fig. S7).

Analysis of the T cell populations (fig. S7) revealed no changes in $CD4^+$ and $CD8^+$ T cell frequencies (fig. S9, A and B), confirming our findings in mice. The frequency of TIM3 (T cell immunoglobulin domain and mucin domain-3) and/or PD-1 (programmed cell death protein 1)–expressing $CD4^+$ or $CD8^+$ T cells (fig. S9, C and D) and $CD4^+CD25^+CD127^-Foxp3^+$ regulatory T cells (fig. S9E) was higher in patients when compared to healthy controls. The percentage

Figure 2. Chemotherapy normalizes systemic tumor-induced myeloid subsets, while intratumoral T cells are not affected.

(**A**) C57BL/6 mice were injected with TC-1 tumor cells (TC-1) and treated with HPV16 $E7_{43-77}$ peptide in Montanide vaccine (V) in the flank opposite of the tumor and with carboplatin (C) and paclitaxel (P) as indicated in the schematic diagram. (**B**) Flow cytometry analysis of the total percentage of myeloid cells (left; column 2 *vs* 1 (p=0.007), 4 (p=0.003) and 5 (p<0.0001)), the $CD11b^+/Gr\text{-}1^{hi}$ cells (middle; column 2 *vs* 1 (p=0.0004), 3, (p=0.03), 4 and 5 (p<0.0001); column 3 *vs* 4 (p=0.02) and 5 (p=0.002)) and the $CD11b^+/Gr\text{-}1^{int}$ (right) cells in the blood (B). (**C**) Representative flow cytometry plots for each treatment, gated on live ($7AAD^-$) cells (top). Distribution of $Gr\text{-}1^{hi}$, $Gr\text{-}1^{int}$ and $Gr\text{-}1^{low}$ expressing cells within the total $CD11b^{hi}$ population is indicated (bottom). Tumor samples (T) were collected and the percentage of (**D**) $CD45^+$ cells within the live gate (Column 1 *vs* 2 and 4 (p<0.0001) and 3 (p=0.02). Column 3 *vs* 2 and 4 (p<0.0001)), (**E**) $CD8^+$ T-cells in the leukocyte gate (Column 1 *vs* 2 and 4 (p<0.0001). Column 3 *vs* 2 and 4 (p<0.0001)), (**F**) vaccine-specific T cells determined by $H2\text{-}D^b$ $E7_{49-57}$ (RAHYNIVTF) tetramer staining (Column 1 *vs* 2 and 4 (p<0.0001). Column 3 *vs* 2 and 4 (p<0.0001)) are depicted. (**G**) Single cell suspensions of tumors were co-incubated with HPV16 $E7_{43-77}$ peptide-pulsed D1 cells and stained intracellular for TNFα and IFN-γ. Representative flow cytometry plots (left) and quantification (right) of the frequency of cytokine producing $CD8^+$ T cells (IFN-γ graph: column 1 *vs* 2 (p=0.009) and 4 (p=0.0001); column 3 *vs* 2 (p=0.004) and 4 (p<0.0001). TNFα graph: column 1 *vs* 2 (p=0.006) and 4 (p=0.0009); column 3 *vs* 2 (p=0.008) and 4 (p=0.001)). N=5-7 mice per group, data shown is representative of two individual experiments. Data is expressed as mean plus SEM and analyzed by one-way ANOVA followed by Tukey's post-hoc analysis.

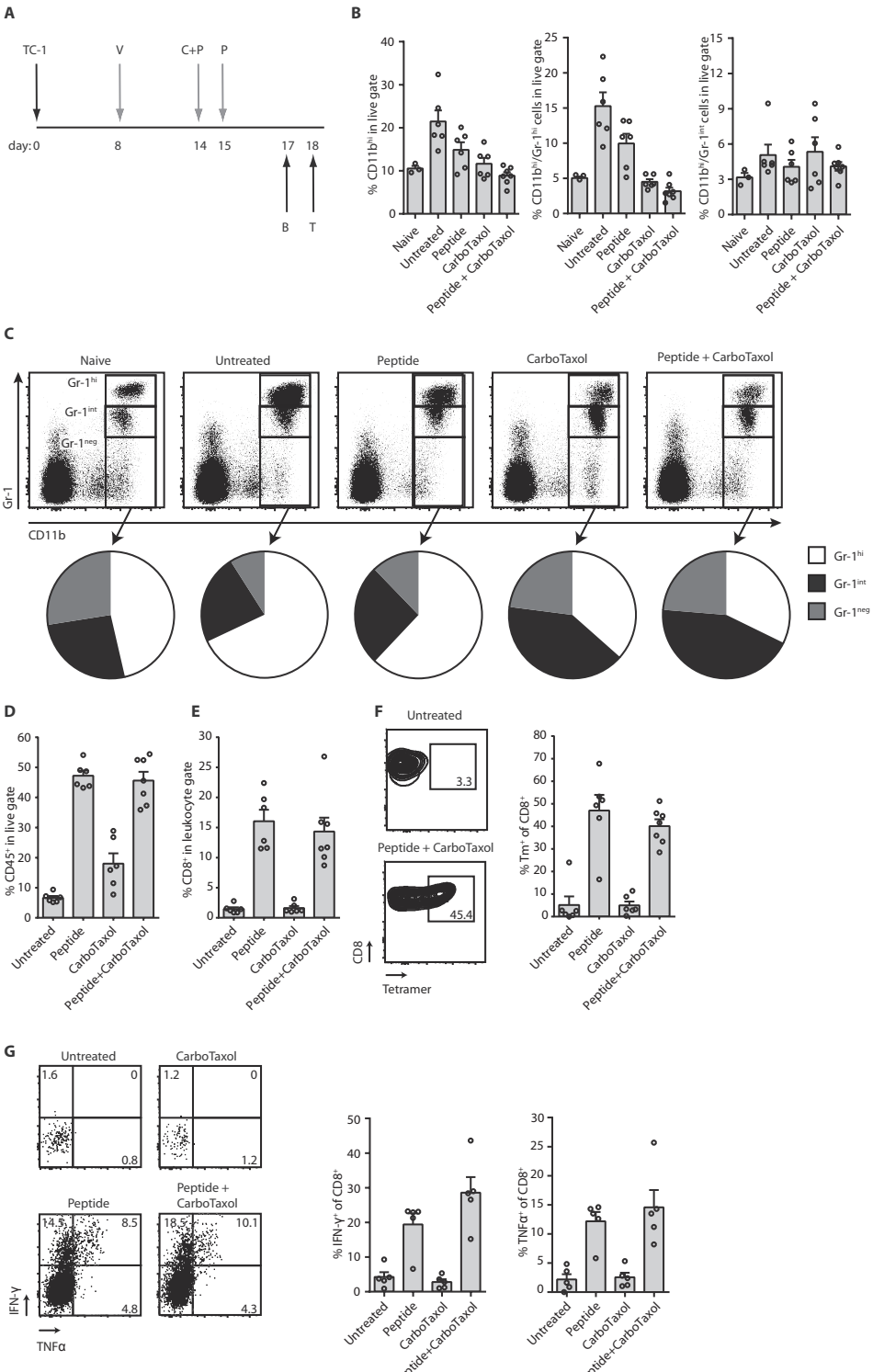
A
TC-1
V
C+P
P
day: 0
8
14
15
17
18
B
T
B
% CD11b^hi in live gate
% CD11b^hi/Gr-1^hi cells in live gate
% CD11b^hi/Gr-1^int cells in live gate
Naive
Untreated
Peptide
CarboTaxol
Peptide + CarboTaxol
C
Naive
Untreated
Peptide
CarboTaxol
Peptide + CarboTaxol
Gr-1^hi
Gr-1^int
Gr-1^neg
Gr-1
CD11b
D
% CD45^+ in live gate
E
% CD8^+ in leukocyte gate
F
Untreated
3.3
Peptide + CarboTaxol
45.4
CD8
Tetramer
% Tm^+ of CD8^+
G
Untreated
CarboTaxol
Peptide
Peptide + CarboTaxol
1.6
0
0.8
1.2
0
1.2
14.5
8.5
4.8
18
10.1
4.3
IFN-γ
TNFα
% IFN-γ^+ of CD8^+
% TNFα^+ of CD8^+

of $CD4^+TIM3^+PD1^-$ and that of regulatory T cells slightly decreased during chemotherapy (fig. S9, C and E).

Together, these results showed that CarboTaxol treatment strongly affected myeloid cells but not lymphocytes. CarboTaxol treatment normalized the amounts of different myeloid cell populations found to be increased in the blood of cervical cancer patients. This normalization of myeloid cell numbers coincided with improved T cell reactivity to antigens from common pathogens, suggesting a relief from general immunosuppression.

Timed vaccination during chemotherapy results in a strong and sustained HPV16-specific T cell response

Twelve patients received a single vaccination with the HPV16-SLP vaccine (8, 10, 11) at 2 weeks (13 to 17 days) after the second (n = 11) or third cycle of chemotherapy (n = 1; ID6008). None of the patients had a demonstrable preexisting response to HPV16 E6/E7. Vaccination with the HPV16-SLP vaccine induced proliferative T cell responses in 11 patients (Fig. 7A). The median stimulation index to all six peptide pools was 25.0 (range, 4.3 to 133.4) at 3 weeks after vaccination in these responders. Vaccine-induced HPV16-specific proliferation was retained after six cycles of chemotherapy and even increased in some cases (median, 21.0; range, 5.0 to 141.5; Fig. 7A, black bars versus gray bars). The vaccine-specific proliferative T cell response in the seven $HPV16^+$ patients was not statistically higher than in the other patients (Fig. 7B). For six patients, enough PBMCs were available to analyze the vaccine-induced T cell response by intracellular staining for IFN-γ, IL-2 (interleukin-2), and TNFα. A polyfunctional cytokine response to HPV16 E6 was measured in five and to E7 in four of the six patients. One patient (ID6004) was anergic (fig. S10), confirming the results of the proliferation assay (Fig. 7A).

Previously, patients with recurrent $HPV16^+$ cervical cancer were vaccinated at least 1 month after chemotherapy (11). In comparison to the responses seen during the earlier trial, the proliferative responses obtained by vaccination during chemotherapy were of far greater magnitude (fig. S11).

Figure 3. Gr-1^{hi} cells are depleted from the tumor by CarboTaxol treatment.
Mice were treated as in Fig. 2. Tumor samples were isolated and analyzed by flow cytometry. (**A**) Leukocytes from resected untreated tumors were analyzed for the expression of Gr-1 and CD11b. The expression of class II, CD80, CD86, F4/80, Ly6G and CD11c on the Gr-1^{hi} (grey lines) and Gr-1^{int} (black lines) subsets. (**B**) Four days after chemotherapy or ten days after peptide vaccination leukocytes of resected tumors were analyzed for the expression of Gr-1 and CD11b (top). Distribution of Gr-1^{hi}, Gr-1^{int} and Gr-1^{low} expressing cells within the total $CD11b^{hi}$ population (bottom). (**C**) Percentages (mean plus SEM) of Gr-1^{hi} (Column 1 *vs* 2 (p=0.006), 3 (p=0.0004) and 4 (p=0.0008)) and Gr-1^{int} (Column 4 *vs* 1 (p=0.0006) and 2 (p=0.02)) subsets was analyzed for untreated and treated tumors. N=5-7 mice per group, data shown is representative of two individual experiments. Data is analyzed by one-way ANOVA followed by Tukey's post-hoc analysis.

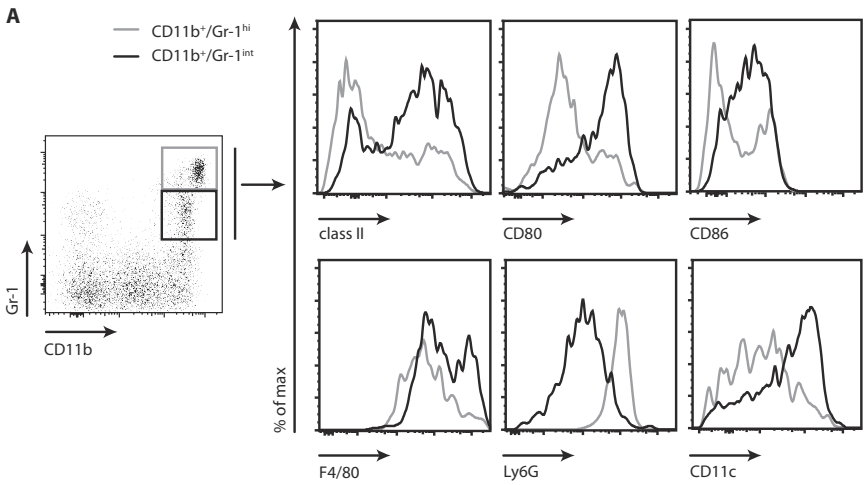
A
CD11b+/Gr-1hi
CD11b+/Gr-1int
Gr-1
CD11b
% of max
class II
CD80
CD86
F4/80
Ly6G
CD11c

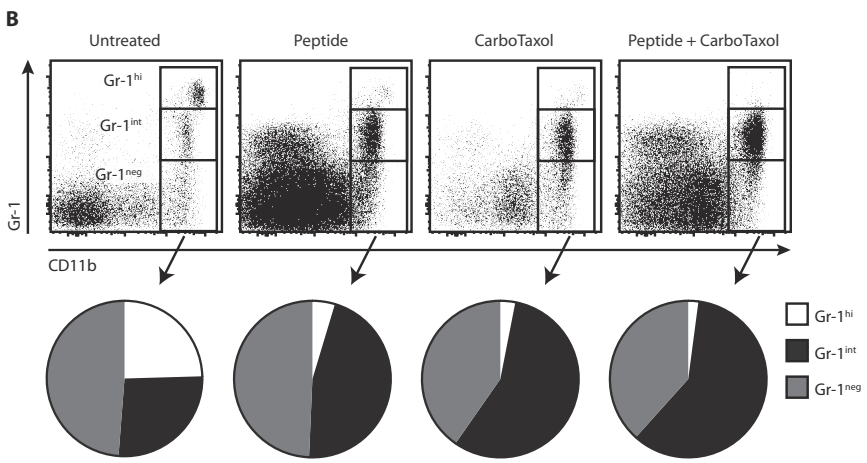
B
Untreated
Peptide
CarboTaxol
Peptide + CarboTaxol
Gr-1hi
Gr-1int
Gr-1neg
Gr-1
CD11b

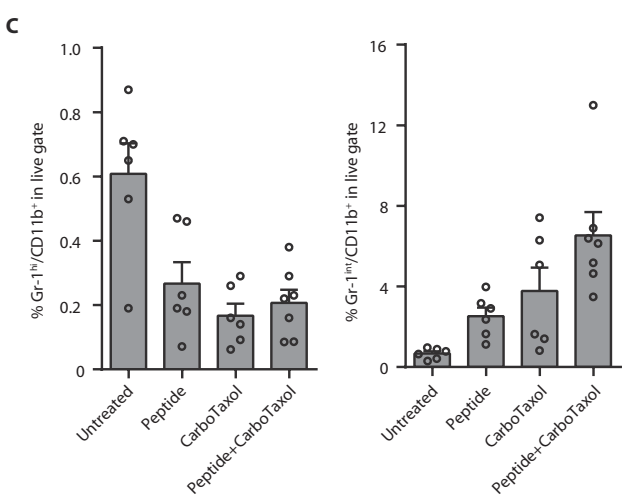
C
% Gr-1hi/CD11b+ in live gate
% Gr-1int/CD11b+ in live gate
Untreated
Peptide
CarboTaxol
Peptide+CarboTaxol

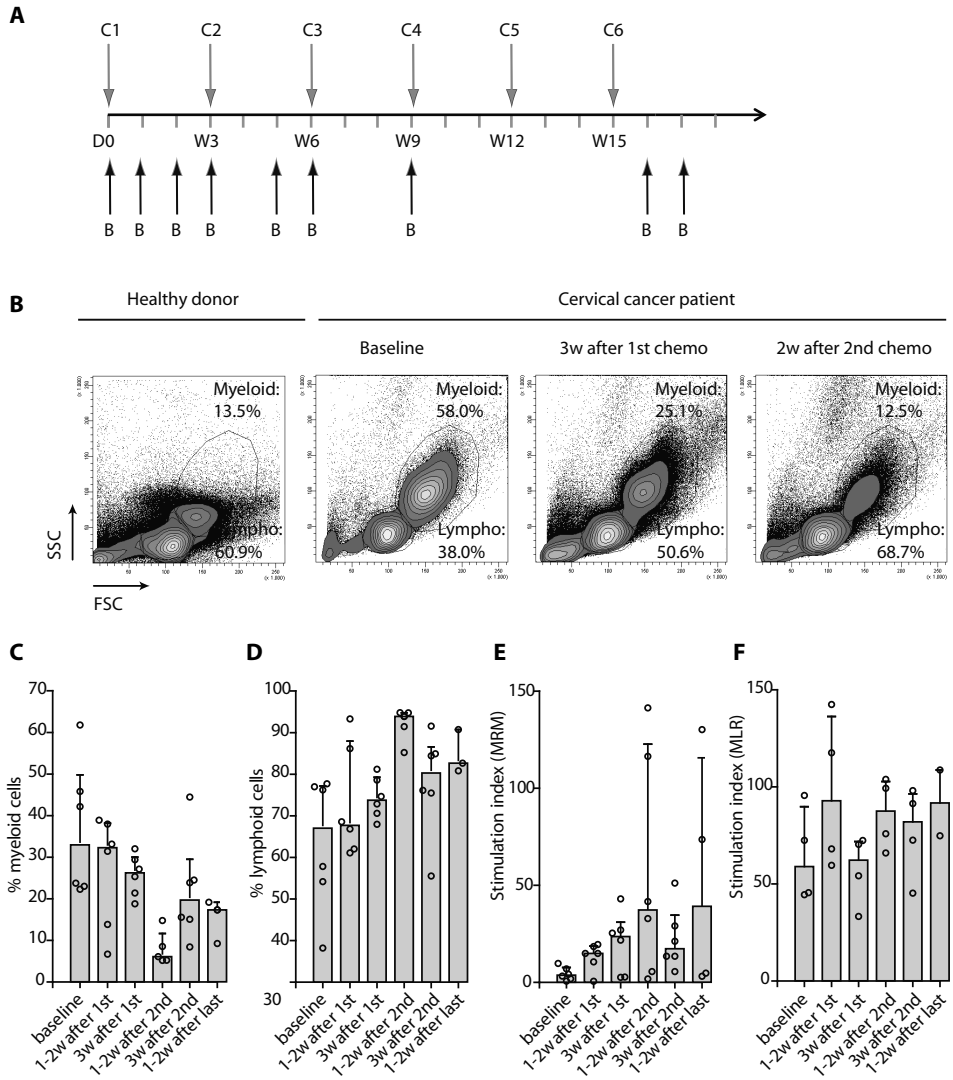

Figure 4. CarboTaxol induces changes in cellular immunity in advanced stage cervical cancer patients.
(**A**) Blood draws (B) and CarboTaxol cycles (C) of the 6 patients in cohort 1 are indicated in days (D) and weeks (W) in the schematic outline. (**B**) Representative flow cytometry plots showing the myeloid cell gate and lymphocyte gate in blood of a patient at baseline and after 1-2 CarboTaxol cycles in comparison to the blood of a healthy donor. The percentage myeloid cells and lymphoid within the total number of cells is indicated. To determine the relative percentage of each population, the sum of the events in the lymphoid and myeloid cell gates in the forward and side scatter plots was set to 100 and then the frequency of (**C**) myeloid cells (column 1 *vs* 4 (p=0.0002), 5 (p=0.02) and 6 (p=0.005)) and of (**D**) lymphocytes (column 1 *vs* 4 (p=0.0002), 5 (p=0.02) and 6 (p=0.005)) was determined. (**E**) Proliferation of T cells upon recognition of recall antigens (memory response mix) shown as stimulation index. Column 1 *vs* 3 and 6 (p=0.02), 4 (p=0.001) and 5 (p=0.005). (**F**) The ability of antigen presenting cells to stimulate T cells in a mixed lymphocyte reaction shown for the 4 tested patients. Column 1 *vs* 2 (p=0.005) and 4 (p=0.049). Data (shown as median plus interquartile range) is analyzed by repeated measures model.

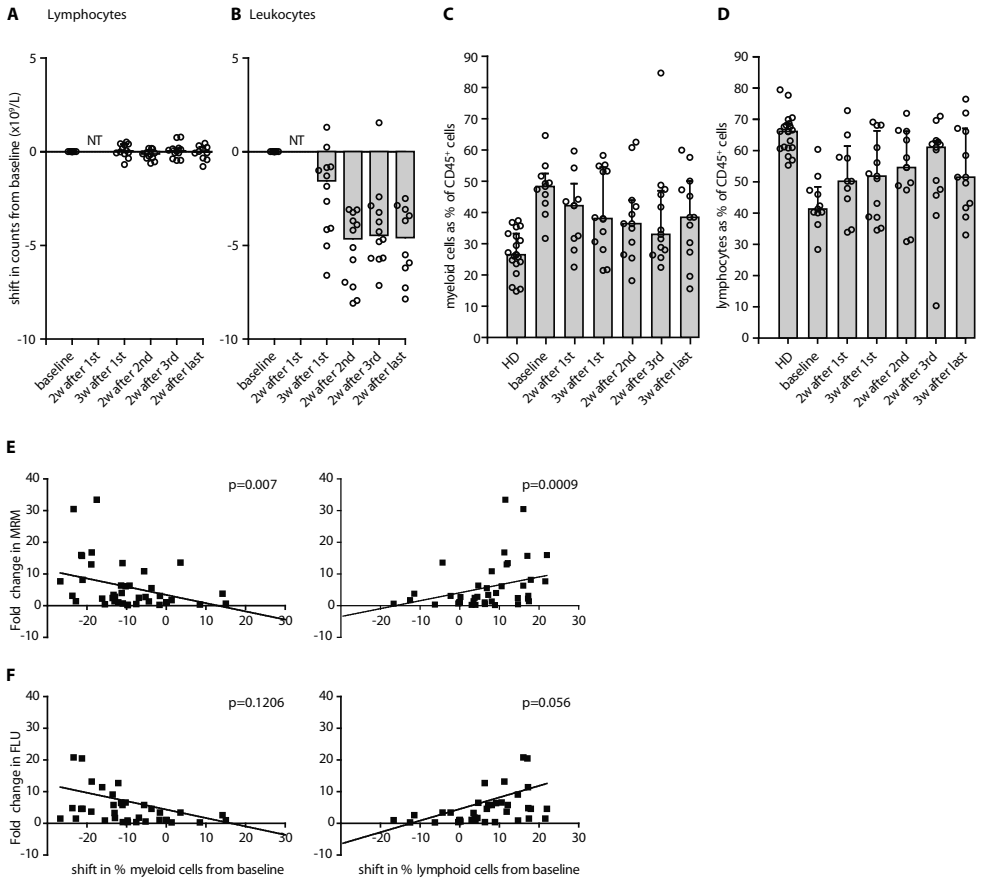

Figure 5. The levels of circulating immune cells normalize upon CarboTaxol treatment.
Blood samples of the 12 patients of cohort 2 were analyzed for leukocyte differentiation showing the shift from baseline for the counts of (**A**) lymphocytes and (**B**) leukocytes x10^9/L. Column 1 *vs* 3 (p=0.007) and 4 to 6 (p<0.0001). Column 3 *vs* 4 (p<0.0001), 5 (p=0.04) and 6 (p=0.003). The frequency of (**C**) myeloid cells (Column 1 *vs* 2 (p<0.0001), 3 (p=0.002), 4 (p=0.003), 5 (p=0.006), 6 (p=0.008) and 7 (p=0.009); column 2 *vs* 3 (p=0.04), 4 (p=0.02), 5 (p=0.007), 6 and 7 (p=0.004)) and (**D**) lymphocytes (Column 1 *vs* 2 (p<0.0001), 3 (p=0.0004), 4 (p=0.0009), 5 (p=0.002), 6 (p=0.005) and 7 (p=0.006); column 2 *vs* 3 (p=0.02), 4 (p=0.002), 5 (p=0.0009), 6 and 7 (p=0.0002)) were determined in the forward and side scatter plots of these blood samples after acquisition by flow cytometry. Blood samples from healthy donors (n=19) were included for comparison. Data (shown as median plus interquartile range) is analyzed by repeated measures model. The fold change in stimulation index (SI), which is SI in a sample during/after chemotherapy divided by that of the baseline sample, of the blood samples stimulated with (**E**) recall antigens (MRM) or (**F**) Influenza Matrix 1 peptides (FLU) is shown versus the shift in percentage of myeloid or lymphoid cells from baseline. Repeated measures regression analysis is conducted to determine whether there is a slope significantly different from 0, represented with the p-value.

Myeloid cell depletion improves the response of PBMCs to stimulation *in vitro*

To recapitulate *in vitro* the association between a reduced myeloid cell population and improved T cell reactivity to recall antigens and HPV16 vaccination, we depleted myeloid cells

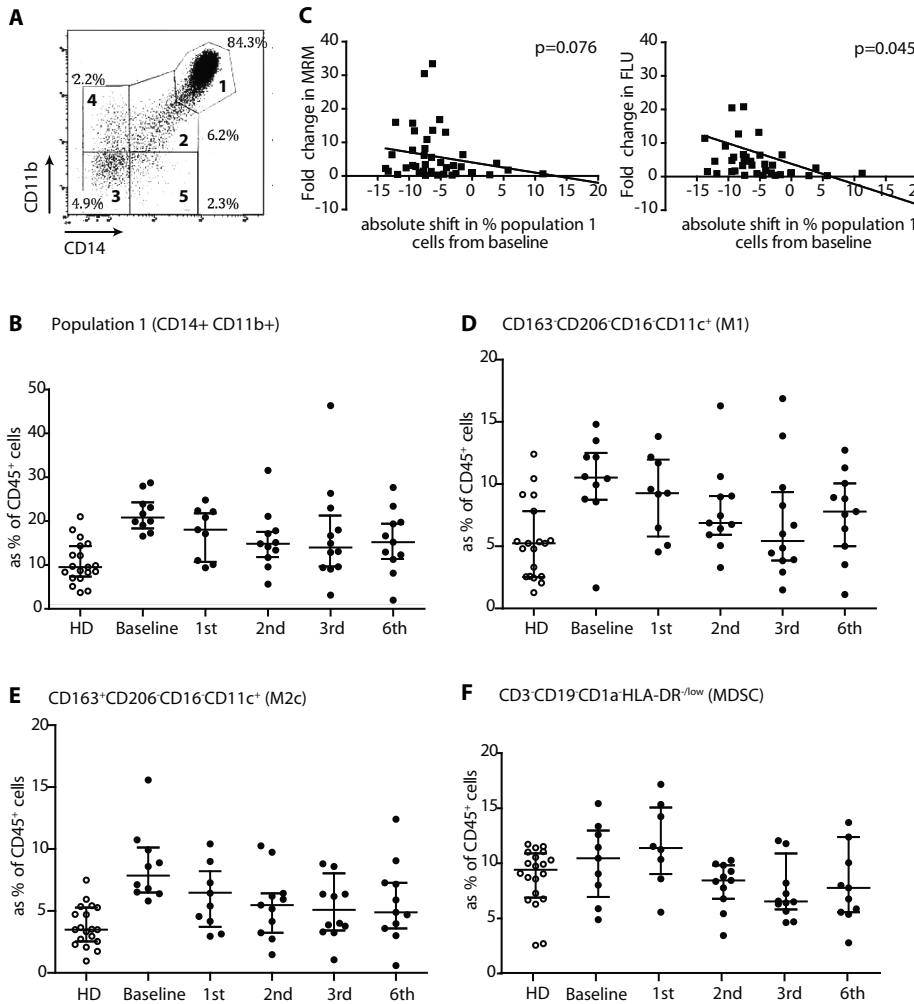

Figure 6. CarboTaxol treatment induces a decline in all subsets of circulating myeloid cells.
PBMC from the 12 patients in cohort 2 were subjected to multi-parameter flow cytometry analysis. (**A**) Representative dot plots of the five subpopulations within the $CD45^+CD3^-CD19^-CD1a^-HLA\text{-}DR^+$ population defined by expression of CD11b and CD14 in the baseline blood sample and 2 weeks after the second cycle of chemotherapy. (**B**) The frequency of ($CD45^+CD3^-CD19^-CD1a^-HLA\text{-}DR^+$) $CD11b^+CD14^+$ (population 1) as percentage of the $CD45^+$ cells in healthy donors (HD, N=19) and the patients over time. The time point of blood sampling (x-axis) was 2 weeks after the first (1^{st}), second (2^{nd}), third (3^{rd}) and 3 weeks after the sixth (6^{th}) or last chemotherapy cycle. Column 1 *vs* 2 (p<0.0001), 3 (p=0.01), 4 (p=0.02), 5 (p=0.009) and 6 (p=0.04). Column 2 *vs* 3 (p=0.04), 4 (p=0.01), 5 (p=0.02) and 6 (p=0.005). (**C**) The fold change in stimulation index (SI) of the blood samples stimulated with recall antigens (MRM) or Influenza Matrix 1 peptides (FLU) is shown versus the absolute shift in percentage of population 1 cells from baseline. Repeated measures regression analysis is conducted to determine whether there is a slope significantly different from 0, represented with the p-value. The frequency of (**D**) $CD163^-CD206^-CD16^-CD11c^+$ (M1-like cells; column 1 *vs* 2 (p=0.001) and 3 (p=0.01); column 2 *vs* 5 (p=0.01)) and (**E**) $CD163^+CD206^-CD16^-CD11c^+$ (M2c-like cells; column 1 *vs* 2 (p=0.004) and 5 (p=0.01)) within population 1 are shown for the healthy donors and patients over time. (**F**) The frequency of myeloid-derived suppressor cells ($CD45^+CD3^-CD19^-CD1a^-HLA\text{-}DR^{-/low}$) is depicted. Column 1 *vs* 3 (p=0.03). Column 2 *vs* 4 (p=0.04). Data (shown as median plus interquartile range) is analyzed by repeated measures model.

from the PBMCs of two patients displaying relatively high frequencies of myeloid cells before chemotherapy and stimulated these PBMCs with autologous monocytes pulsed with a mix of recall antigens, a mix of E6 and E7 peptides, or a mix of p53 peptides as control for 11 days before the antigen-specific T cell response was tested. As a control, we used nondepleted PBMCs. Not only was the T cell response to recall antigens much higher in the culture started with myeloid cell–depleted PBMCs, but the HPV16-specific response was also more efficiently boosted during these 11 days. As expected, no reactivity was detected in the cultures stimulated with the control p53 peptides (fig. S12).

Combination of chemotherapy with vaccination is safe in advanced cervical cancer patients

Safety was assessed according to the Common Terminology Criteria for Adverse Events (CTCAE) v3.0. Most of the observed adverse events (AEs) were disease-related or chemotherapy-related. All patients developed chemotherapy-related anemia, thrombocytopenia, leucopenia, neutropenia, and alopecia. There were seven AEs, all in different patients, related to the advanced stage of the disease: shortness of breath, pulmonary embolism, abdominal pain (lymphedema), gastroenteritis, erysipelas, hydronephrosis. One patient (ID6002) died before vaccination could take place, and one patient (ID6004) died 11 weeks after vaccination. The cause of death in both cases was progressive disease. Vaccine-related AEs were largely localized to the vaccination site (table S2). One patient developed an ulcer at the injection site, which persisted for more than 6 weeks and required antibiotic treatment.

DISCUSSION

Here, we observed that tumors expressing the HPV16 oncoproteins E6 and E7 cause the numbers of circulating myeloid cells to be abnormally high in TC-1–challenged mice and in HPV-positive cervical cancer patients. Treatment with CarboTaxol normalizes the numbers of circulating myeloid cells but has no negative effect on the number and function of lymphocytes. In mice, CarboTaxol treatment had a similar effect on the myeloid cell composition within the tumors as in the blood. The effects of CarboTaxol are, therefore, not limited to circulating immune cells, and it is likely that similar effects occur within the tumors of cervical cancer patients. The CarboTaxol-mediated normalization of circulating myeloid cells was associated with increased T cell–mediated tumor control in mice and with higher T cell reactivity against common microbial recall antigens and response to HPV16-SLP vaccination in patients. This suggests a causal relationship between the normalization of abnormally high myeloid cell frequencies and improved T cell responsiveness. Because the combination of HPV16-SLP vaccination plus CarboTaxol improved the cure rate of mice with established TC-1 tumors, we expect that the robust and sustained HPV16-specific T cell responses seen with this combination improve the efficacy of treatment in patients with advanced cervical cancer. This needs to be studied in a future randomized clinical trial.

CarboTaxol is a standard chemotherapeutic treatment not only in cervical cancer but also in patients with other cancer types, including lung cancer and ovarian cancer. Its effect on the immune system, however, has not been widely studied. Carboplatin and paclitaxel

are both known to cause dose-limiting myelotoxicity (22, 23). This is likely a direct effect on precursor cells in the bone marrow, as observed in different animal models (24). White bone marrow cells display impaired *in vitro* capacity to proliferate when treated with carboplatin (25). Furthermore, the number of myeloid cells reaching its nadir at 2 weeks and a rebound at 3 weeks after CarboTaxol treatment is in line with the mechanistic models for the development and maturation of leukocytes and drug susceptibility in the bone marrow (26, 27). Lymphopenia has not been reported. We observed an increase in T cell reactivity 1 to 2 weeks after the second and subsequent cycles of chemotherapy. This was not a result of changes in absolute lymphocyte counts or strong alterations in the number or phenotype of $CD4^+$, $CD8^+$, or regulatory T cells. Similar observations were made in ovarian cancer patients. Those patients who responded to CarboTaxol displayed a stronger IFN-γ–producing $CD8^+$ T cell response during treatment 12 to 14 days after chemotherapy (28, 29). Here, we show that the positive effect of CarboTaxol on the immune response results from the normalization of abnormal myeloid cell numbers, which are initially high in the presence of larger tumor burden. Leukocytosis has been described in patients and animals with HPV-associated cancers (30, 31), but the composition of the increased leukocyte populations was not analyzed in detail. An in-depth analysis of the myeloid cell subsets affected by CarboTaxol revealed that these effects were found across all subsets that are elevated in patients or in tumor-bearing animals. This includes tumor growth–suppressing myeloid cells, but more importantly the tumor-promoting myeloid cell populations, which can suppress the function of antitumor effector T cells. Apparently, the balance among these subsets and in particular the decline in immunosuppressive myeloid cells within the tumor microenvironment appears to be important for successful implementation of immunotherapy and improved clinical efficacy. The change in the proportions of myeloid cells and lymphocytes allowed the latter population to respond to antigenic stimulation, most likely through a relief from myeloid cell–mediated immunosuppression. This notion is sustained by the unexpectedly high proliferative responses after timed application of a single vaccination and our *in vitro* experiment showing that removal of excessive $CD14^+$ myeloid cells from prechemotherapy PBMC samples of two cancer patients allowed the tumor-specific T cells to react to antigenic stimulation. This seems to be a general phenomenon, and we observed this also in the context of lung cancer (20). A recent phase II trial in patients with extensive small-cell lung cancer reported that ipilimumab treatment beginning with the third cycle of CarboTaxol produced better clinical outcomes than giving the drugs during cycles 1 to 4 (32). The effect of CarboTaxol

Figure 7. HPV16 SLP vaccination during CarboTaxol treatment results in a strong immune response in patients. The patients in cohort 2 received a single vaccination with the HPV16-SLP subcutaneously at 2 weeks after the second cycle of chemotherapy. (**A**) The proliferative responses of T cells, in the lymphocyte stimulation test (LST), is shown as a stimulation index and depicted versus the indicated peptide pools used for stimulation of the cells in the blood sample at baseline (hatched bar), 2 weeks after second cycle of chemotherapy and prior to vaccination (white bar), 3 weeks after this single vaccination (black bar) and 3 weeks after the sixth or last cycle of chemotherapy (grey bar). (**B**) The patients are grouped by HPV16 status (HPV16+, N=7; HPV16-, N=5) and the proliferative response (stimulation index) is plotted versus the indicated blood samples. Each dot represents one response against HPV16 E6 and E7. In total 6 peptide pools were tested per blood sample. Data is analyzed by linear mixed model analysis and showed no statistical significance.

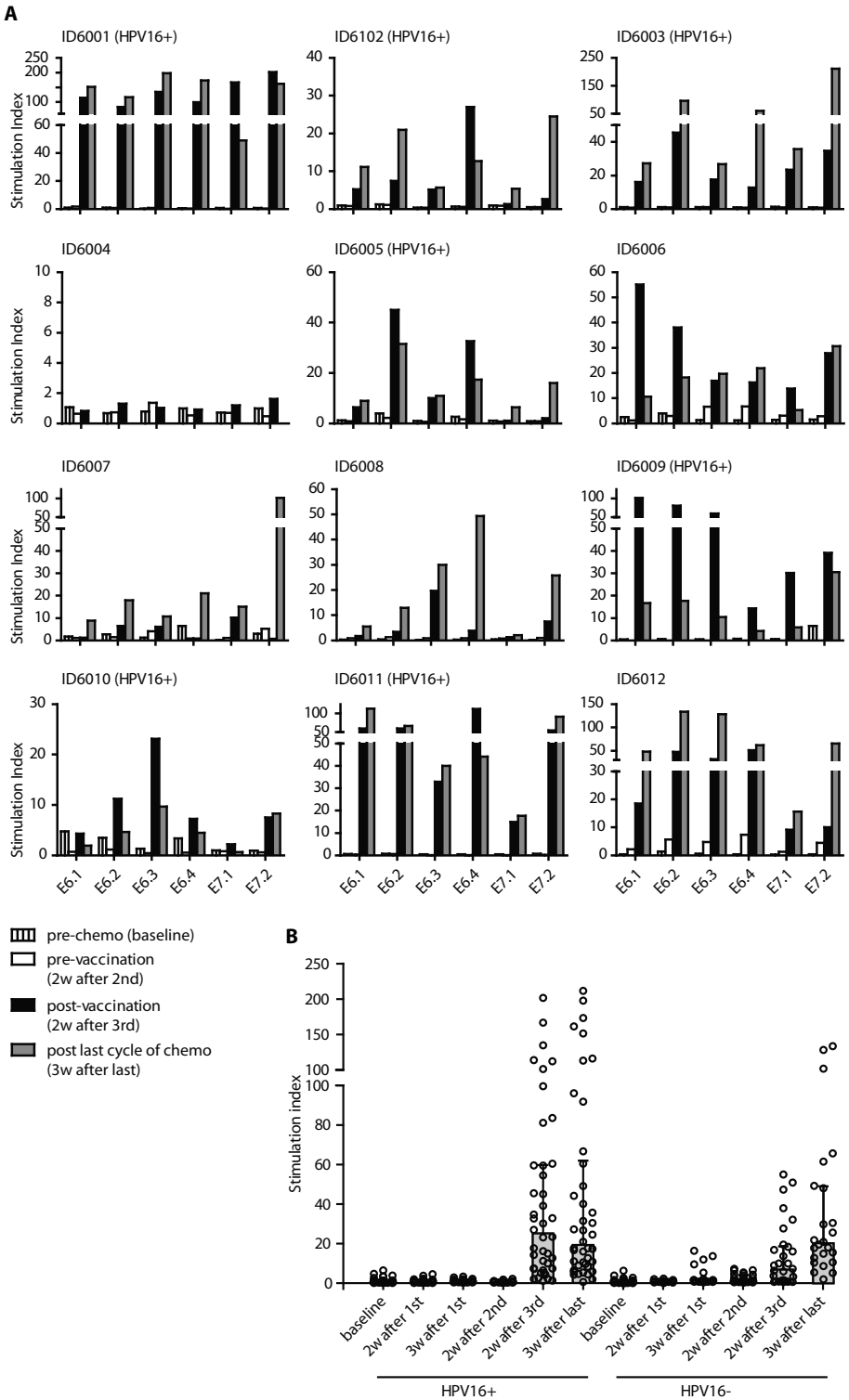
A
ID6001 (HPV16+)
ID6102 (HPV16+)
ID6003 (HPV16+)
ID6004
ID6005 (HPV16+)
ID6006
ID6007
ID6008
ID6009 (HPV16+)
ID6010 (HPV16+)
ID6011 (HPV16+)
ID6012
Stimulation Index
E6.1
E6.2
E6.3
E6.4
E7.1
E7.2
pre-chemo (baseline)
pre-vaccination (2w after 2nd)
post-vaccination (2w after 3rd)
post last cycle of chemo (3w after last)
B
Stimulation index
baseline
2w after 1st
3w after 1st
2w after 2nd
2w after 3rd
3w after last
HPV16+
HPV16-

on myeloid cells may have relieved myeloid cell–mediated suppression of T cells, as in our study, providing ipilimumab the opportunity to release the brakes on activated T cells in the later phase of treatment. The effects of CarboTaxol on myeloid cells are clear in patients with cancers where myeloid cells have prognostic value (33, 34), of which cervical and ovarian carcinomas are prime examples. Other types of cancer in which myeloid cells play an important immunosuppressive and prognostic role are thus also candidates for timed immunotherapy.

Our study has some limitations. First, although abnormal numbers of myeloid cells are found both in the mouse model and in patients, their phenotype differs. In mice, the chemotherapy-related reduction in circulating $CD11b^{hi}Gr\text{-}1^{hi}$ cells reflected their depletion in the tumor. In patients, a number of circulating myeloid cell subsets were reduced, but whether this also occurs in the tumor remains to be established. Second, in comparison to the T cell responses obtained in our earlier studies, the current ones were of far greater magnitude. Although the tests were performed by the same laboratory according to the same standard operating procedures, we did not perform a formal head-to-head comparison, and future trials should confirm these findings. Finally, both the strength of the vaccine-induced immune response and the reduction in circulating myeloid cells were retained for up to 2 weeks after the sixth cycle of CarboTaxol. It is not clear if stopping chemotherapy will coincide with a quick rebound of the myeloid cells, how this affects the vaccine-induced immune response, and whether the phenotype of myeloid cells will be altered under the influence of vaccine-activated T cells. These should all be subjects of future investigations.

In conclusion, we have shown that CarboTaxol chemotherapy not only is devoid of immunosuppressive effects on tumor-specific T cells but also vigorously stimulates tumor-specific immunity by normalizing the abnormal numbers of the immunosuppressive myeloid cell populations. Additional studies will have to demonstrate whether CarboTaxol and adequately timed HPV16-SLP vaccination also produce clinical benefit in patients with advanced cervical cancer. A larger clinical trial is already under way to test this (NCT02128126). If successful, this immunotherapeutic approach should be easy to implement because it combines smoothly with the preferred chemotherapy treatment for advanced cervical cancer.

REFERENCE LIST

1. Ho GY, Kadish AS, Burk RD, Basu J, Palan PR, Mikhail M, et al. HPV 16 and cigarette smoking as risk factors for high-grade cervical intra-epithelial neoplasia. Int J Cancer 1998;78:281-5.
2. Burke TW, Hoskins WJ, Heller PB, Shen MC, Weiser EB, Park RC. Clinical patterns of tumor recurrence after radical hysterectomy in stage IB cervical carcinoma. Obstet Gynecol 1987;69:382-5.
3. Larson DM, Copeland LJ, Stringer CA, Gershenson DM, Malone JM, Jr., Edwards CL. Recurrent cervical carcinoma after radical hysterectomy. Gynecol Oncol 1988;30:381-7.
4. Monk BJ, Sill MW, McMeekin DS, Cohn DE, Ramondetta LM, Boardman CH, et al. Phase III trial of four cisplatin-containing doublet combinations in stage IVB, recurrent, or persistent cervical carcinoma: a Gynecologic Oncology Group study. J Clin Oncol 2009;27:4649-55.
5. Lorusso D, Petrelli F, Coinu A, Raspagliesi F, Barni S. A systematic review comparing cisplatin and carboplatin plus paclitaxel-based chemotherapy for recurrent or metastatic cervical cancer. Gynecol Oncol 2014;133:117-23.
6. zur HH. Papillomaviruses and cancer: from basic studies to clinical application. Nat Rev Cancer 2002;2:342-50.
7. van der Burg SH, Melief CJ. Therapeutic vaccination against human papilloma virus induced malignancies. Curr Opin Immunol 2011;23:252-7.
8. Kenter GG, Welters MJ, Valentijn AR, Lowik MJ, Berends-van der Meer DM, Vloon AP, et al. Vaccination against HPV-16 oncoproteins for vulvar intraepithelial neoplasia. N Engl J Med 2009;361:1838-47.
9. van Poelgeest MI, Welters MJ, Vermeij R, Stynenbosch LF, Loof NM, Berends-van der Meer DM, et al. Vaccination against Oncoproteins of HPV16 for Noninvasive Vulvar/Vaginal Lesions: Lesion Clearance Is Related to the Strength of the T-Cell Response. Clin Cancer Res 2016;22:2342-50.
10. Welters MJ, Kenter GG, de Vos van Steenwijk PJ, Lowik MJ, Berends-van der Meer DM, Essahsah F, et al. Success or failure of vaccination for HPV16-positive vulvar lesions correlates with kinetics and phenotype of induced T-cell responses. Proc Natl Acad Sci U S A 2010;107:11895-9.
11. van Poelgeest MI, Welters MJ, van Esch EM, Stynenbosch LF, Kerpershoek G, van Persijn van Meerten EL, et al. HPV16 synthetic long peptide (HPV16-SLP) vaccination therapy of patients with advanced or recurrent HPV16-induced gynecological carcinoma, a phase II trial. J Transl Med 2013;11:88.
12. Hanahan D, Weinberg RA. The hallmarks of cancer. Cell 2000;100:57-70.
13. Bracci L, Schiavoni G, Sistigu A, Belardelli F. Immune-based mechanisms of cytotoxic chemotherapy: implications for the design of novel and rationale-based combined treatments against cancer. Cell Death Differ 2014;21:15-25.
14. van der Sluis TC, van Duikeren S., Huppelschoten S, Jordanova ES, Beyranvand Nejad E., Sloots A, et al. Vaccine-induced tumor necrosis factor-producing T cells synergize with cisplatin to promote tumor cell death. Clin Cancer Res 2015;21:781-94.
15. Diaz Y, Tundidor Y, Lopez A, Leon K. Concomitant combination of active immunotherapy and carboplatin- or paclitaxel-based chemotherapy improves anti-tumor response. Cancer Immunol Immunother 2013;62:455-69.
16. Nowak AK, Robinson BW, Lake RA. Synergy between chemotherapy and immunotherapy in the treatment of established murine solid tumors. Cancer Res 2003;63:4490-6.
17. Lin KY, Guarnieri FG, Staveley-O'Carroll KF, Levitsky HI, August JT, Pardoll DM, et al. Treatment of established tumors with a novel vaccine that enhances major histocompatibility class II presentation of tumor antigen. Cancer Res 1996;56:21-6.
18. de JA, van Poelgeest MI, van der Hulst JM, Drijfhout JW, Fleuren GJ, Melief CJ, et al. Human papillomavirus type 16-positive cervical cancer is associated with impaired CD4+ T-cell immunity against early antigens E2 and E6. Cancer Res 2004;64:5449-55.
19. Dijkgraaf EM, Santegoets SJ, Reyners AK, Goedemans R, Wouters MC, Kenter GG, et al. A phase I trial combining carboplatin/doxorubicin with tocilizumab, an anti-IL-6R monoclonal antibody, and interferon-alpha2b in patients with recurrent epithelial ovarian cancer. Ann Oncol 2015;26:2141-9.

20. Talebian YM, Loof NM, Franken KL, Taube C, Oostendorp J, Hiemstra PS, et al. Local and systemic XAGE-1b-specific immunity in patients with lung adenocarcinoma. Cancer Immunol Immunother 2015;64:1109-21.

21. Walter S, Weinschenk T, Reinhardt C, Singh-Jasuja H. Single-dose cyclophosphamide synergizes with immune responses to the renal cell cancer vaccine IMA901. Oncoimmunology 2013;2:e22246.

22. Nabholtz JM, Gelmon K, Bontenbal M, Spielmann M, Catimel G, Conte P, et al. Multicenter, randomized comparative study of two doses of paclitaxel in patients with metastatic breast cancer. J Clin Oncol 1996;14:1858-67.

23. Yarbro CH. Carboplatin: a clinical review. Semin Oncol Nurs 1989;5:63-9.

24. Rose WC, Schurig JE. Preclinical antitumor and toxicologic profile of carboplatin. Cancer Treat Rev 1985;12 Suppl A:1-19.

25. Treskes M, Boven E, van de Loosdrecht AA, Wijffels JF, Cloos J, Peters GJ, et al. Effects of the modulating agent WR2721 on myelotoxicity and antitumour activity in carboplatin-treated mice. Eur J Cancer 1994;30A:183-7.

26. Minami H, Sasaki Y, Saijo N, Ohtsu T, Fujii H, Igarashi T, et al. Indirect-response model for the time course of leukopenia with anticancer drugs. Clin Pharmacol Ther 1998;64:511-21.

27. Krzyzanski W, Jusko WJ. Multiple-pool cell lifespan model of hematologic effects of anticancer agents. J Pharmacokinet Pharmacodyn 2002;29:311-37.

28. Coleman S, Clayton A, Mason MD, Jasani B, Adams M, Tabi Z. Recovery of CD8+ T-cell function during systemic chemotherapy in advanced ovarian cancer. Cancer Res 2005;65:7000-6.

29. Wu X, Feng QM, Wang Y, Shi J, Ge HL, Di W. The immunologic aspects in advanced ovarian cancer patients treated with paclitaxel and carboplatin chemotherapy. Cancer Immunol Immunother 2010;59:279-91.

30. Mabuchi S, Matsumoto Y, Isohashi F, Yoshioka Y, Ohashi H, Morii E, et al. Pretreatment leukocytosis is an indicator of poor prognosis in patients with cervical cancer. Gynecol Oncol 2011;122:25-32.

31. Stone SC, Rossetti RA, Bolpetti A, Boccardo E, Souza PS, Lepique AP. HPV16-associated tumors control myeloid cell homeostasis in lymphoid organs, generating a suppressor environment for T cells. J Leukoc Biol 2014;96:619-31.

32. Reck M, Bondarenko I, Luft A, Serwatowski P, Barlesi F, Chacko R, et al. Ipilimumab in combination with paclitaxel and carboplatin as first-line therapy in extensive-disease-small-cell lung cancer: results from a randomized, double-blind, multicenter phase 2 trial. Ann Oncol 2013;24:75-83.

33. de Vos van Steenwijk PJ, Ramwadhdoebe TH, Goedemans R, Doorduijn EM, van Ham JJ, Gorter A, et al. Tumor-infiltrating CD14-positive myeloid cells and CD8-positive T-cells prolong survival in patients with cervical carcinoma. Int J Cancer 2013;133:2884-94.

34. Wouters M, Dijkgraaf EM, Kuijjer ML, Jordanova ES, Hollema H, Welters M, et al. Interleukin-6 receptor and its ligand interleukin-6 are opposite markers for survival and infiltration with mature myeloid cells in ovarian cancer. Oncoimmunology 2014;3:e962397.

SUPPLEMENTAL INFORMATION

Analysis of murine tumor infiltrating immune populations

TC-1 tumor-bearing mice were injected with synthetic long HPV16 $E7_{43-77}$ peptide in the contralateral flank. Chemotherapy was provided intraperitoneally (i.p.) on day 14 (carboplatin) and day 14 and 15 (paclitaxel). On day 17 blood was taken and analyzed by flow cytometry. Tumor infiltrating immune populations were analyzed as previously described (*13*). Briefly, single cell suspensions of tumors of transcardially perfused mice were incubated with 7-Aminoactinomycin D (for dead cell exclusion, Life Technologies), with H-$2D^b$ tetramers containing HPV16 $E7_{49-57}$ peptide (RAHYNIVTF) labeled with APC and indicated antibodies from Biolegend: Gr-1-PE Cy7 (clone RB6-8C5)), Ly6G-Alexa Fluor 700 (AF700; clone 1A8), CD4-BV605 (clone L3T4) and eBioscience:, CD11b-Pacific Blue (PC; clone M1/70)), F4/80-PE (clone Bm8), CD80-FITC (clone 16-10A1), CD86-PE (clone GL1, BD), CD3-PE Cy7 (clone 145-2C11), CD8a-AF700 (clone 53-6.7), CD45.2 eFluor 780 (clone 104) and CD19-APC (clone 1D3), or BD: MHC-class II-Horizon V500 (HV500; clone M5/114.15.2, BD), CD11c Brilliant Violet 605 (BV605; clone HL3, BD).

To determine the capacity of cells to produce pro-inflammatory cytokines, single cell suspensions of tumor (-infiltrates) were incubated for 5 hours with 40,000 D1 dendritic cells pre-loaded with HPV16 $E7_{43-77}$ peptide (10 μg/ml) in the presence of Brefeldin A (2 μg/ml, Sigma). After cell surface staining with fluorescently labelled antibodies to mouse CD45, CD8 and CD3, overnight fixation with 0.5% paraformaldehyde solution (Pharmacy LUMC) and permeabilization with Perm/Wash buffer (BD) cells were stained at 4˚C with antibodies against IFN-γ (APC, clone XMG1.2, eBioscience) and TNFα (FITC, clone MP6-XT22, eBioscience).

Immunomonitoring of blood samples from cervical cancer patients

The sample

Venous blood samples (45 mL in heparinized tubes and 8.5 mL in clot activator tube) were taken for immunomonitoring prior to chemotherapy (baseline), 1 or 2 weeks after the first cycle of chemotherapy (1-2wk after 1st), prior to (3wk after 1st) and 1-2 weeks after the second cycle (1-2wk after 2nd), 2-3 weeks after the 3rd cycle (2-3wk after 3rd) and 1-2 or 3 weeks after the in Table S1 indicated last cycle (which is maximal 6th cycle; 1-2 or 3w after last) of chemotherapy (Fig. 4A). In addition, from 19 healthy blood donor volunteers (≥18 years old females) a blood sample (50 mL) was drawn after they had signed an informed consent. The blood (transported at room temperature) was processed within 3 hours and peripheral blood mononuclear cells (PBMCs) were isolated by Ficoll gradient centrifugation, washed, partly used in the lymphocyte stimulation test (LST) and the remaining cells were cryopreserved (in 90% fetal calf serum (PAA Laboratories) and 10% DMSO at concentration of 7-12 million cells per vial in total volume of 1 mL) using a Mr. Frosty's freezing container (Nalgene). Upon cryopreservation the vials were stored in the vapor phase of the liquid nitrogen until further use.

The assays

Proliferation assays

The HPV16-specific proliferative response was determined using freshly isolated PBMCs that were subjected to the LST as described previously (*8-11*). In short, eight replicate wells with 1.5 x 10^5 cells per well were stimulated for 6 days with HPV16 E6 or E7 peptide pools (10 μg/mL per peptide), after which 50 μL supernatant per well was harvested and stored at -20°C for cytokine analysis. The cells were pulsed with [^{3}H]-Thymidine (Perkin Elmer) for 16 hours, harvested and uptake was determined by the Wallac Microbetatrilux (Perkin Elmer). As a positive control the previously described memory response mix (MRM) and influenza matrix 1 protein-derived overlapping peptides (FLU) were used (*13*). The negative control consist of cells in medium only. A positive response is defined as an stimulation index (SI) of at least 3 under the condition that 6 out of the 8 wells displayed values above the cut off value which was defined as the mean value of the cells in medium only plus 3 x standard deviation (SD).

The capacity to respond to phytohaemagglutinin (PHA) was studied using cryopreserved PBMCs. Cells were thawed and tested in a 3-days proliferation assay as described previously (*33*) with the minor alteration that now 50,000 cells per well (in quadruplicate) were incubated in medium (IMDM, Lonza) or stimulated with 0.5 μg/mL PHA (Murex Biotech HA16). A positive response is defined as an SI of at least 3.

The antigen presenting capacity of the PBMC samples from the patients were determined in a mixed lymphocyte reaction (MLR) *(34)*. Patient's PBMC were thawed in Iscove's Modified Dulbecco's Medium (IMDM) plus 10% fetal bovine serum and 30 μg/ml DNase, resuspended in IMDM plus 10% human AB serum, irradiated (3000 rad) to prevent proliferation, washed and resuspended in IMDM plus 10% human AB serum and then plated at 1 x 10^5 cells per well (in quadruplicate). Third party PBMCs were added (1 x 10^5 million cells/well) making a total volume of 200 μL/well. Irradiated PBMCs only as well as third party PBMCs only were taken along as negative controls. At day 6, 100 μL supernatant per well was harvested for cytokine analysis, and the cells were subjected to [^{3}H]-Thymidine (50 μL/well of 10 μCi/mL) for an additional 16 hours. A positive response is defined as an SI of at least 3.

Myeloid cell depletion and stimulation of PBMC *in vitro*

The CD14+ myeloid cells in PBMC of 2 cervical cancer patients were depleted by magnetic cell sorting (Miltenyi) as described earlier (*28*). Depleted and non-depleted PBMC were stimulated for 11 days with autologous monocytes pulsed with either a mix of FLU overlapping peptides and MRM (*9-11*), a mix of HPV16 E6/E7 SLP (32-35 amino acid long overlapping peptides (*33*)), or a mix of p53 SLP (30-mer overlapping peptides) and then tested in a proliferation test (triplicate wells) as described above in which non-pulsed autologous monocytes served as a negative control (*28*).

Cytokine analysis

The supernatants of the LST, PHA and MLR proliferation assays were used for cytokine analysis by use of flow cytometer based cytokine bead array (CBA, human Th1/Th2 kit, BD) according to the manufacturer's instructions and reported earlier (*9-11*). The cytokines measured by this

kit are IFN-γ, TNFα, IL-10, IL-5, IL-4 and IL-2. A positive response is defined when above the detection limit, which is 20 pg/mL for each of the cytokines. A three-fold increase above the baseline sample (pre-treatment) was defined as a treatment related change.

Phenotyping of PBMCs

The PBMC samples isolated at different time points during treatment were phenotyped using 4 sets of 6-11 cell surface markers to identify macrophages, myeloid derived suppressor cells (MDSC), the expression of co-inhibitory molecules and regulatory T cells by flow cytometry *(34)*.

The macrophage set consists of CD3-PB (Clone UCHT1; Dako), CD1a-FITC (Clone HI149; BD), CD11b-PE (Clone D12; BD), CD11c-AF700 (Clone B-Ly6; BD), CD14-PE Cy7 (Clone M5E2; BD), CD16-PE CF594 (Clone 3G8; BD), CD19-BV605 (BV605, Clone SJ25C1, BD), CD45-PerCP Cy5.5 (Clone 2D1, BD), CD163-APC (Clone 215927; R&D), CD206-APC Cy7 (Clone 15-2, Biolegend) and HLA-DR HV500 (Clone L243, BD).

The MDSC set contains the same CD3-PB, CD19-BV605, CD45-PerCP Cy5.5 and HLA-DR HV500 antibodies and additionally CD11b-FITC (Clone CBRM1/5; Biolegend), CD14-AF700 (Clone M5E2; BD), CD15-PE CF594 (Clone W6D3; BD), CD33-PE Cy7 (Clone P67.6; BD). CD34-APC (Clone 581; BD), and CD124-PE (Clone HiL4R-M57; BD).

The inhibitory set consists of the same antibody for CD3, and additionally CD4-PE CF594 (Clone RPA-T4; BD), CD8-APC Cy7 (Clone SK1, BD), CD152-PE Cy5 (anti-CTLA-4; Clone BN13, BD), CD279-BV605 (anti-PD-1; Clone EH12.2H7, Biolegend) and TIM3-PE (Clone F38-2E2, Biolegend).

The regulatory T cell set consists of CD3-HV500 (Clone UCHT1; BD), CD4-AF700 (Clone RPA-T4; BD), CD8-PerCP Cy5.5 (clone SK1, BD), CD25-PE Cy7 (clone 2A3, BD), CD127-BV650 (clone HIL-7R-M21, BD), FoxP3-PE CF594 (clone 259D/C7, BD), Ki67-FITC (clone 20Raj1, eBioscience), CD45-RA-APC H7 (clone HI100, BD) and live/dead marker (Yellow Amino Reactive Dye (ARD), Life Technologies).

The sets of markers for MDSC and regulatory T cells are according to the consensus within the CIMT immunoguiding program (CIP).

The cryopreserved PBMCs were thawed and stained . Briefly, for the staining of surface markers the cells were washed in phosphate buffered saline (PBS) supplemented with 0.5% Bovine Serum Albumin (BSA, Sigma), incubated for 10 min at RT in PBS/0.5% BSA/10%FCS (in the dark) to prevent non-specific antibody binding, centrifuged and resuspended in the antibody mixtures described above and incubated for 30 min on ice (in the dark). Then, the cells were washed twice with PBS/0.5% BSA and finally resuspended in 1% paraformaldehyde (Pharmacy LUMC). For the regulatory T cell staining, the cells were first subjected to Yellow ARD (20 minutes at room temperature in 100 µL/well of 1:800 diluted Yellow ARD), blocked for non-specific staining and subsequently stained for surface markers as described above, followed by washing in transcription factor fixation and permeabilization buffer (BD) and intranuclear staining with the intranuclear antibodies FoxP3 and Ki67 diluted in permeabilization and washing buffer (BD) for 40-50 minutes at 4°C. The cells were finally resuspended in 1% paraformaldehyde and analysed within 24 hours while keeping at 4°C.

Intracellular cytokine staining (ICS)

For the simultaneous detection of surface markers (CD3, CD4, CD8), activation markers (CD154, CD137) and intracellular cytokines (IFN-γ and IL-2), the PBMCs were subjected to the direct ex-vivo multiparameter flow cytometry assay as described previously (*9*). Cells in medium only and cells stimulated overnight with Staphylococcal Enterotoxin B (2 μg/mL; Sigma) were taken along as negative and positive control, respectively. A positive response was defined as twice above the negative control and at least 10 events in the gate. A vaccine-induced response required an at least 3-fold increase in reactivity compared to baseline sample.

Flow cytometry

The acquisition on the Fortessa or LSRII (BD) flow cytometers was performed <24h after the staining was finished. Analysis was performed by using FlowJo (Tree Star; Version 10) or DIVA software (Version 6.2).

Laboratory environment.

Immunomonitoring of patient's PBMC was performed in the laboratory of the department of Clinical Oncology (LUMC) that operates under research conditions but uses standard operation procedures for all tests, with pre-established definitions of positive responses and using trained personnel. This laboratory has been externally and internally audited according to the reflection paper for laboratories that perform immunomonitoring (*35*) and participated in all proficiency panels of the CIMT Immunoguiding Program (CIP; of which SHvdB and MJPW are steering committee members; http://www.cimt.eu/workgroups/cip/) as well as many of the proficiency panels (including ICS gating and ELISPOT plate reading panels) of the USA-based Cancer Immunotherapy Consortium (CIC of the Cancer Research Institute) to validate its standard operating procedures (SOPs).

Statistical analysis

Survival for differentially treated tumor-bearing mice was compared using the Kaplan-Meier method and the log-rank (Mantel-Cox) test. Statistical analysis of immune parameters in mice were performed by using the one-way ANOVA followed by Tukey's post-hoc analysis. Statistical analysis was performed using GraphPad Prism software (version 6).

The immune responses of patients were analyzed with a repeated measures model with fixed factors group, time and group by time, and repeated time within the patient group. The Kenward-Roger approximation was used to estimate denominator degrees of freedom and model parameters were estimated using the restricted maximum likelihood method. By residual graph it was decided which variables were log transformed before analysis to correct for the expected log-normal distribution of the data. The general group effect was calculated within the model as the average least square means (LSM) over all times of the patients versus the LSM of the healthy donors. If the general group effect was significant ($p<0.05$) the various differences (healthy donors vs time point patients) were calculated. In a separate analysis with patient data only the general time effect within patients was estimated. If the time effect was significant ($p<0.05$) the various differences (between time points within patient group) were

calculated within the original model. The fold change in MRM and FLU and absolute shift in myeloid, lymphoid and population 1 cells was analyzed with a repeated measures regression analysis with a compound structure covariance structure and time as repeated factor within subject. Since the reduction of myeloid cells reached its nadir after 2 cycles of CarboTaxol and was retained throughout the treatment the results of patient ID 6008, receiving the vaccine after the third cycle, were used as if this patient was vaccinated in the same time window as the others. A p-value < 0.05 was considered statistically significant. Statistical analysis was performed using SAS for windows V9.4 (SAS Institute, Inc., Cary, NC, USA). To determine whether a significant difference exists in the proliferative response to the 6 tested HPV16 peptide pools between the patients with a HPV16+ cervical tumor and those with a HPV16 negative (other HPV type) tumor, a mixed linear model with unstructured correlation metric as covariance type was performed using SPSS statistics (version 20). In this model the possible link between the different peptide pools (although biologically unrelated) is incorporated when the peptide pool is taken as an dependent variable.

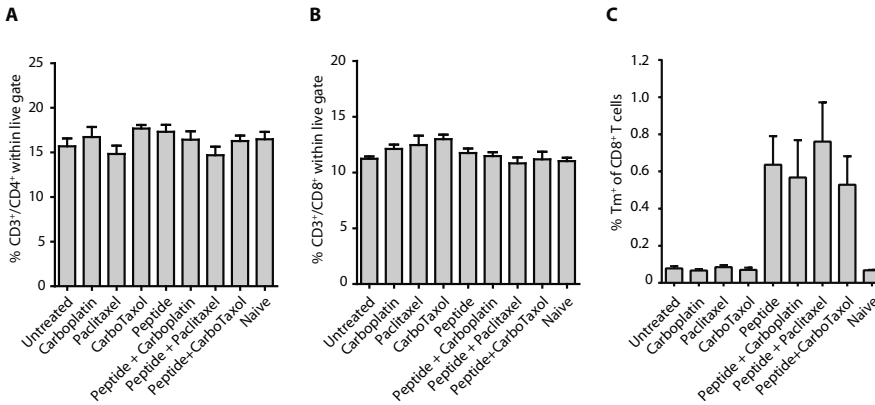

Figure S1. T cells are not affected by CarboTaxol treatment.
Wild-type C57BL/6 mice were injected on day 0 with 1 x 10^5 TC-1 tumor cells. Eight days later, when tumors were palpable, mice were treated systemically with carboplatin (day 8) and paclitaxel (day 8 and 9) with or without addition of synthetic long HPV16 $E7_{43-77}$ peptide in Montanide in the opposite flank. Chemotherapy treatment was repeated one week after initial treatment, vaccination was boosted 14 days after initial treatment. Shown is the quantification of the percentage of (**A**) $CD4^+$ T cells, (**B**) $CD8^+$ T cells and (**C**) the vaccine-specific cells within the $CD8^+$ population as determined by H2-Db $E7_{49-57}$ (RAHYNIVTF) tetramer staining. Column 1 *vs* 7 (p=0.008); column 2 *vs* 7 (p=0.007), column 3 *vs* 7 (p=0.009),column 4 *vs* 7 (p=0.007). N=8 mice in the tumor bearing groups, N=4 in the naïve group, data is representative of two individual experiments and expressed as mean plus SEM. Data is analyzed by one-way ANOVA followed by Tukey's post-hoc analysis.

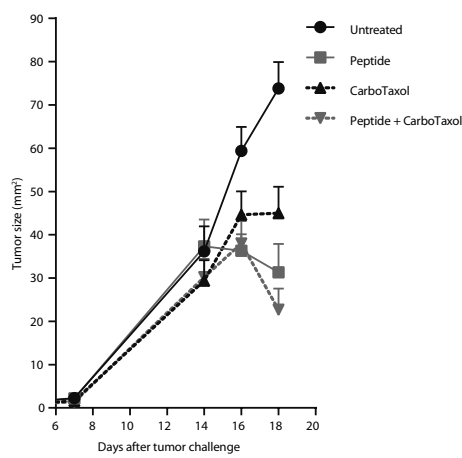

Figure S2. The delay in tumor growth does not differ between the different treatment groups.
Wild-type C57BL/6 were injected with TC-1 tumor cells. Eight days later, when tumors were palpable, mice were treated with synthetic long HPV16 $E7_{43-77}$ peptide in Montanide in the opposite flank. Carboplatin was administered on day 14, paclitaxel on day 14 and 15. Tumor size was measured in time and shown as the mean tumor size measured two-dimensionally (mm^2) plus SEM. Significant differences in tumor size was calculated for day 18 using one-way ANOVA. The tumor size in the untreated group of mice was significantly different from that of the peptide treated mice (p=0.0003), the CarboTaxol treated mice (p=0.01) and from the peptide plus CarboTaxol treated group (p<0.0001), whereas there was no significant difference between the different treatment groups. Experiment was performed with 5-7 mice per group, data shown is representative of two individual experiments.

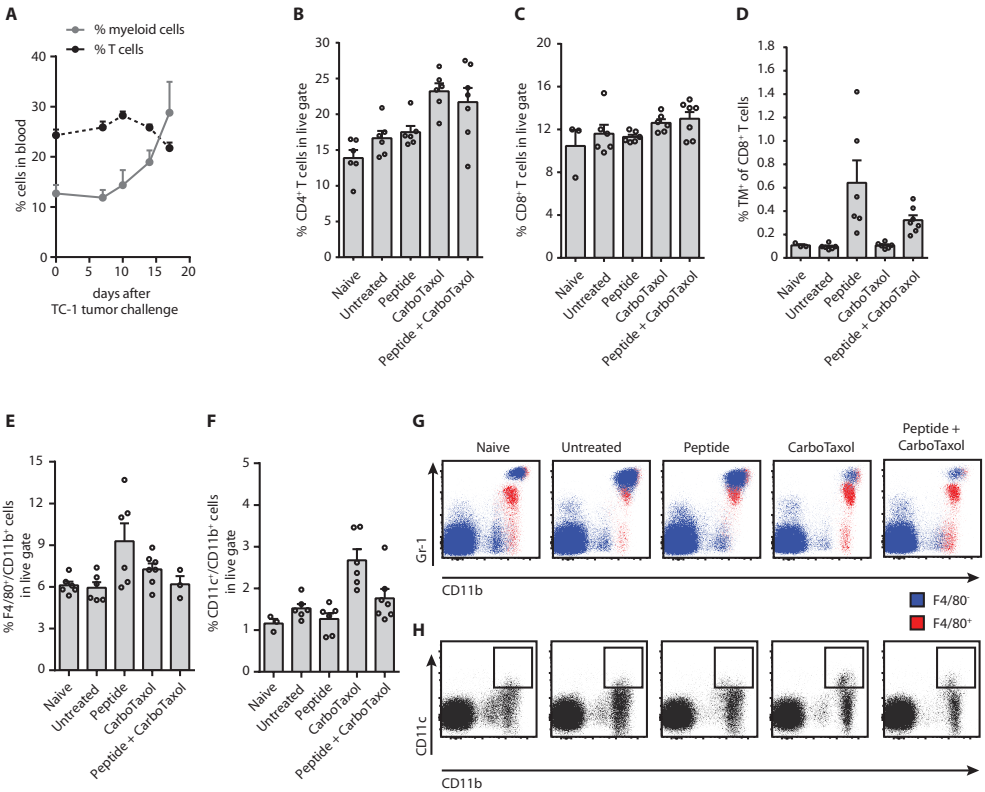

Figure S3. Chemotherapy does not hamper T cells but decreases myeloid cell frequencies.
Wild-type C57BL/6 were injected with TC-1 tumor cells. (**A**) Upon tumor growth and if left untreated the frequency of myeloid cells increased and the percentage of T-cells decreased as measured in the blood of the tumor-bearing mice. In another experiment TC-1 tumor cells were injected. Eight days later, when tumors were palpable, mice were treated systemically with synthetic long HPV16 $E7_{43-77}$ peptide in Montanide in the opposite flank. Carboplatin was administered on day 14, paclitaxel on day 14 and 15. Flow cytometry was used to quantify the percentage (mean plus SEM) of (**B**) $CD4^+$ T cells (Column 1 *vs* 4 (p=0.001) and 5 (p=0.008); column 4 *vs* 2 (p=0.01) and 3 (p =0.04), (**C**) $CD8^+$ T cells, (**D**) the vaccine-specific cells within the $CD8^+$ T-cell population (Column 3 *vs* 1 (p=0.02), 2 (p=0.003) and 4 (p=0.004), (**E**) monocytes (identified as F4/80 and CD11b positive (Column 4 *vs* 2 (p=0.049) and 3 (p=0.03)) and (**F**) dendritic cells (Column 4 *vs* 1 (p=0.002), 2 (p=0.005), 3 (p=0.0008) and 5 (p=0.02). (**G**) Overlay of $F4/80^+$ cells in flow cytometry plots that show Gr-1 and CD11b expression of all live cells in blood of (treated-) mice. (**H**) Flow cytometry plots representing CD11c and CD11b expression of all live cells in blood of (treated-) mice. Experiment was performed with 5-7 mice per group, data shown is representative of two individual experiments. Data is analyzed by one-way ANOVA followed by Tukey's post-hoc analysis.

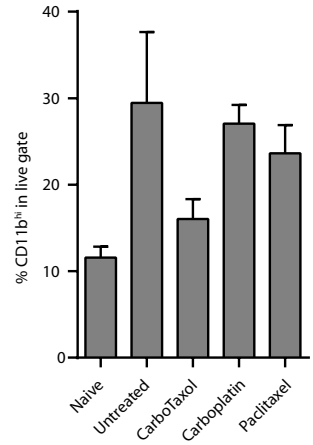

Figure S4. The combination of carboplatin and paclitaxel result in the strongest reduction of circulating myeloid cells.

Wild-type C57BL/6 mice were injected with TC-1 tumor cells. Carboplatin was administered on day 14 and paclitaxel on day 14 and 15. Flow cytometry was used to quantify the percentage of $CD11b^{hi}$ cells in the blood. The experiment was performed with 5 mice per group. Data (shown as mean plus SEM) is analyzed by one-way ANOVA followed by Tukey's post-hoc analysis.

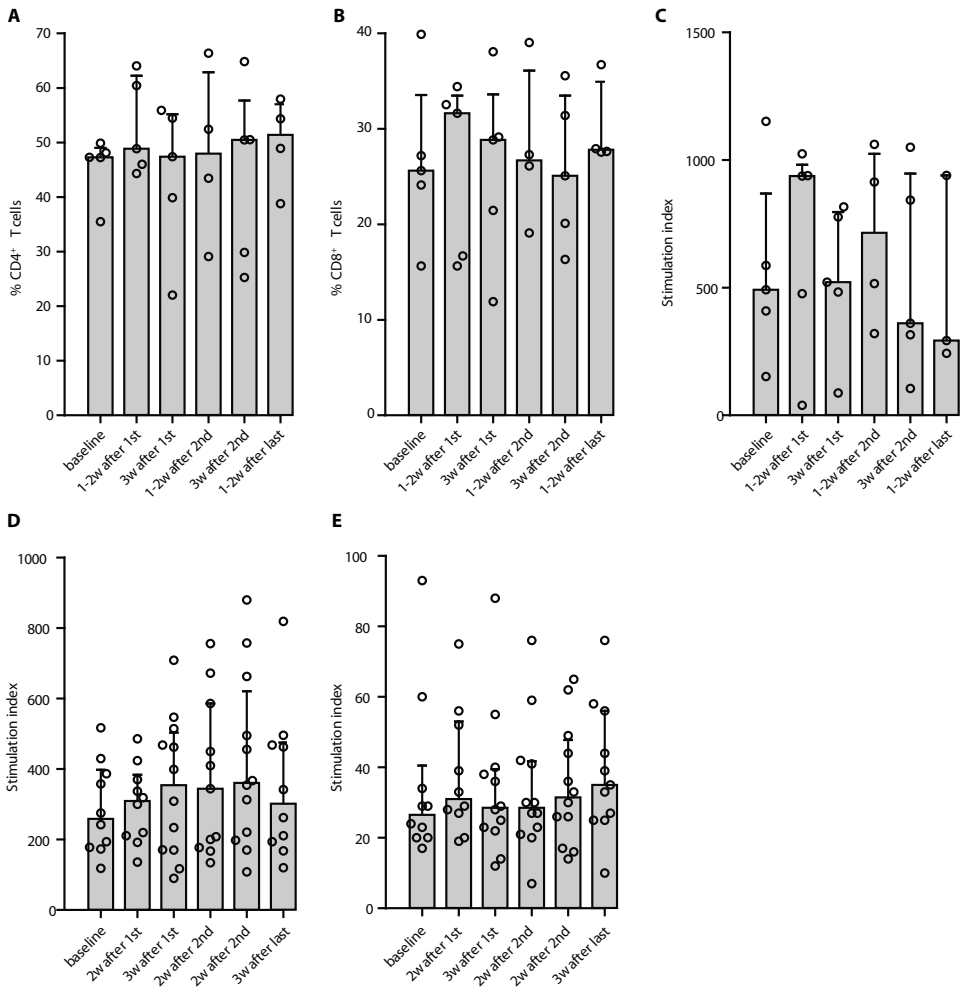

Figure S5. CarboTaxol therapy does not influence general immune parameters.
Blood samples of different time points (prior, during and after chemotherapy) from 5 of the 6 cervical cancer patients in cohort 1 were subjected to flow cytometry to determine the frequency of (**A**) $CD4^+$ and (**B**) $CD8^+$ T cells. Plotted are the percentages of these two types of T cells within the lymphocyte gate. PBMC samples from (**C**) 5 of the 6 patients in cohort 1 and (**D**) the 12 patients in cohort 2 were stimulated with PHA to test their capacity to proliferate. The results are depicted as stimulation index. (**E**) The quality of the antigen presenting cells in the patient's PBMC from cohort 2 were analyzed by mixed lymphocyte reaction. The proliferative capacity of third party PBMC is depicted as stimulation index. Data (shown as median plus interquartile range) is analyzed by repeated measures model.

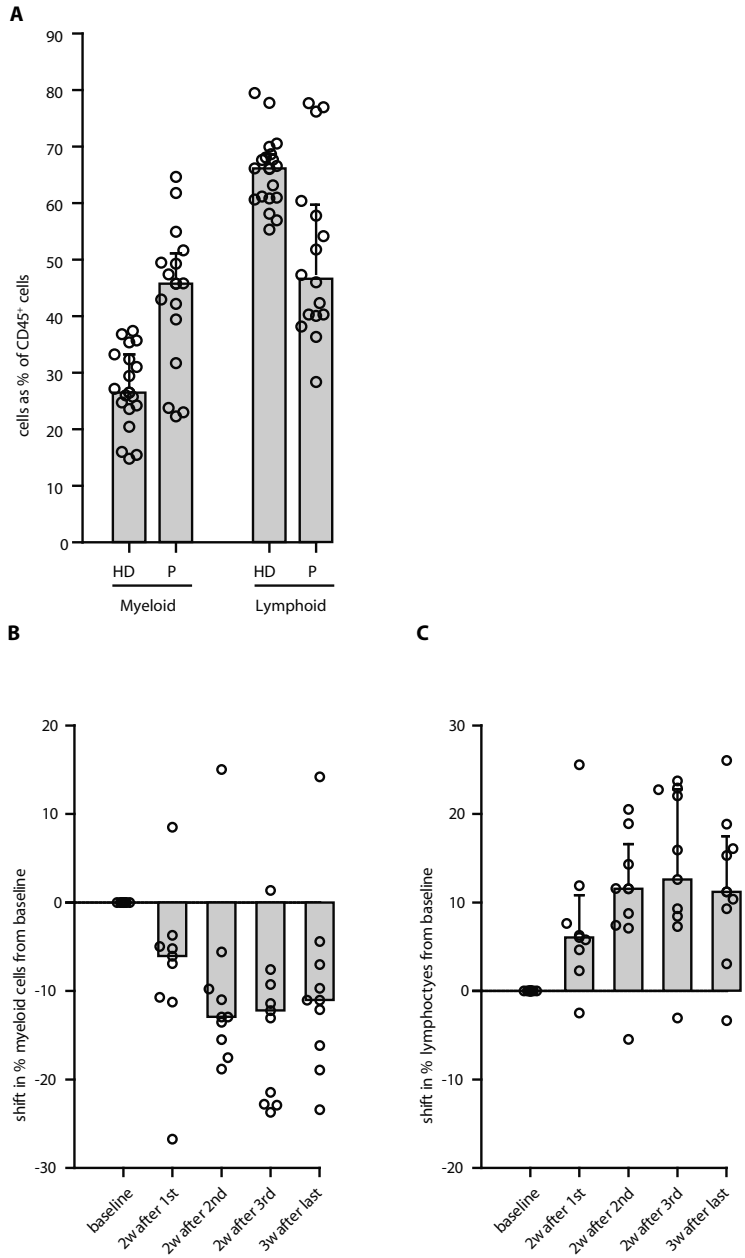

Figure S6. CarboTaxol therapy alters the relative frequencies of myeloid cells and lymphoctyes.
(**A**) The myeloid cells and lymphocytes as percentage of $CD45^+$ cells are depicted for healthy donors (HD, N=19) and cervical cancer patients (P, N=18) at baseline. Column 1 *vs* 2 ($p< 0.0001$); column 3 *vs* 4 ($p<0.0001$). The shifts in the frequency of (**B**) myeloid cells (Column 1 *vs* 2 ($p=0.04$), 3 ($p=0.007$), 4 and 5 ($p=0.004$)) and (**C**) lymphocytes (Column 1 *vs* 2 ($p=0.02$), 3 ($p=0.0009$), 4 and 5 ($p=0.0002$)) compared to baseline values are depicted for the blood samples obtained from the cervical cancer patients of cohort 2 prior to, during and after the last cycle of chemotherapy with CarboTaxol. Data (shown as median plus interquartile range) is analyzed by repeated measures model.

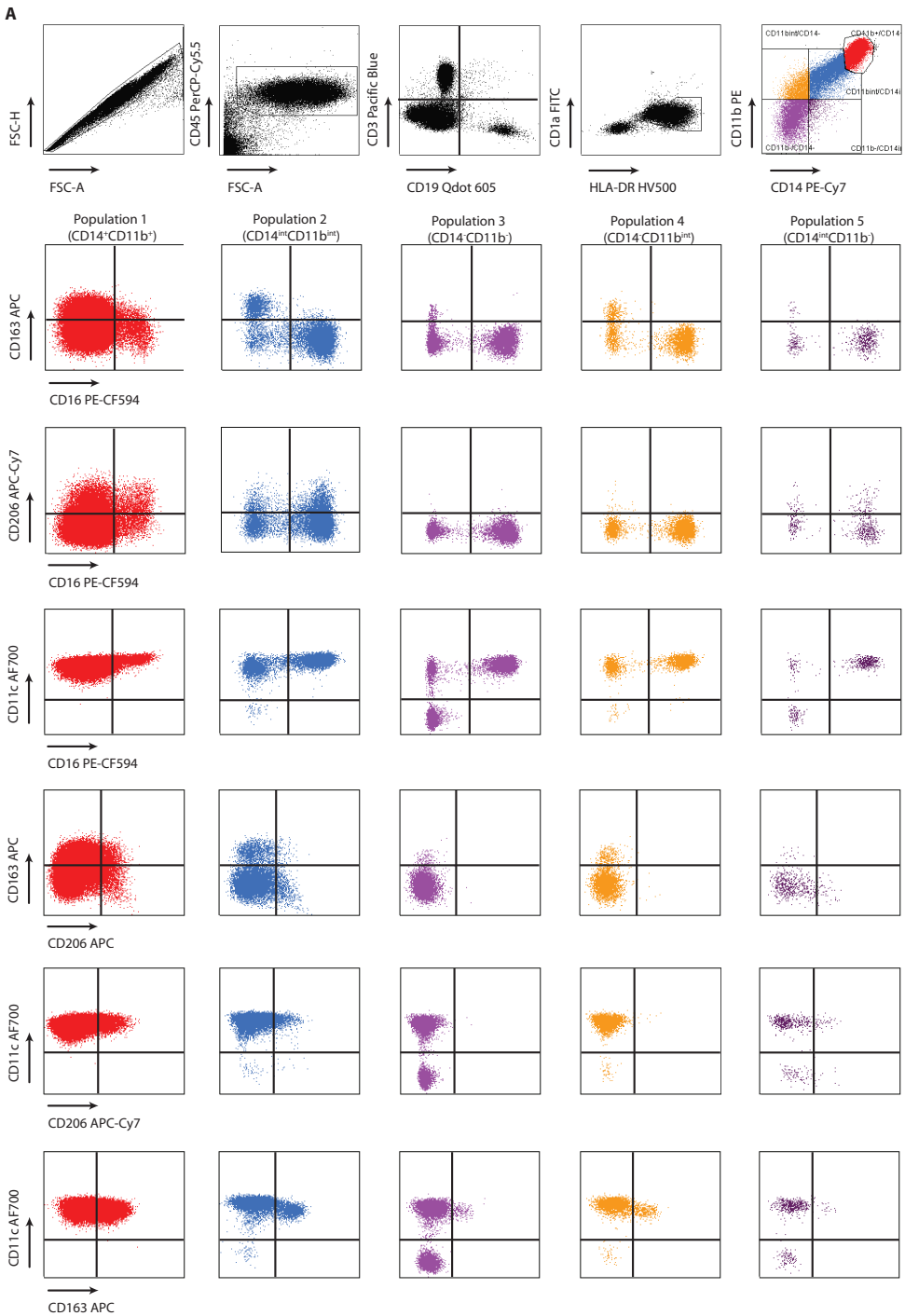

Figure S7. The flow cytometric analysis of myeloid cells and T cells.
Blood samples of the cervical cancer patients are stained for the three different sets of antibodies and acquired by flow cytometry to determine the composition of immune cells within the sample and over time within ▸

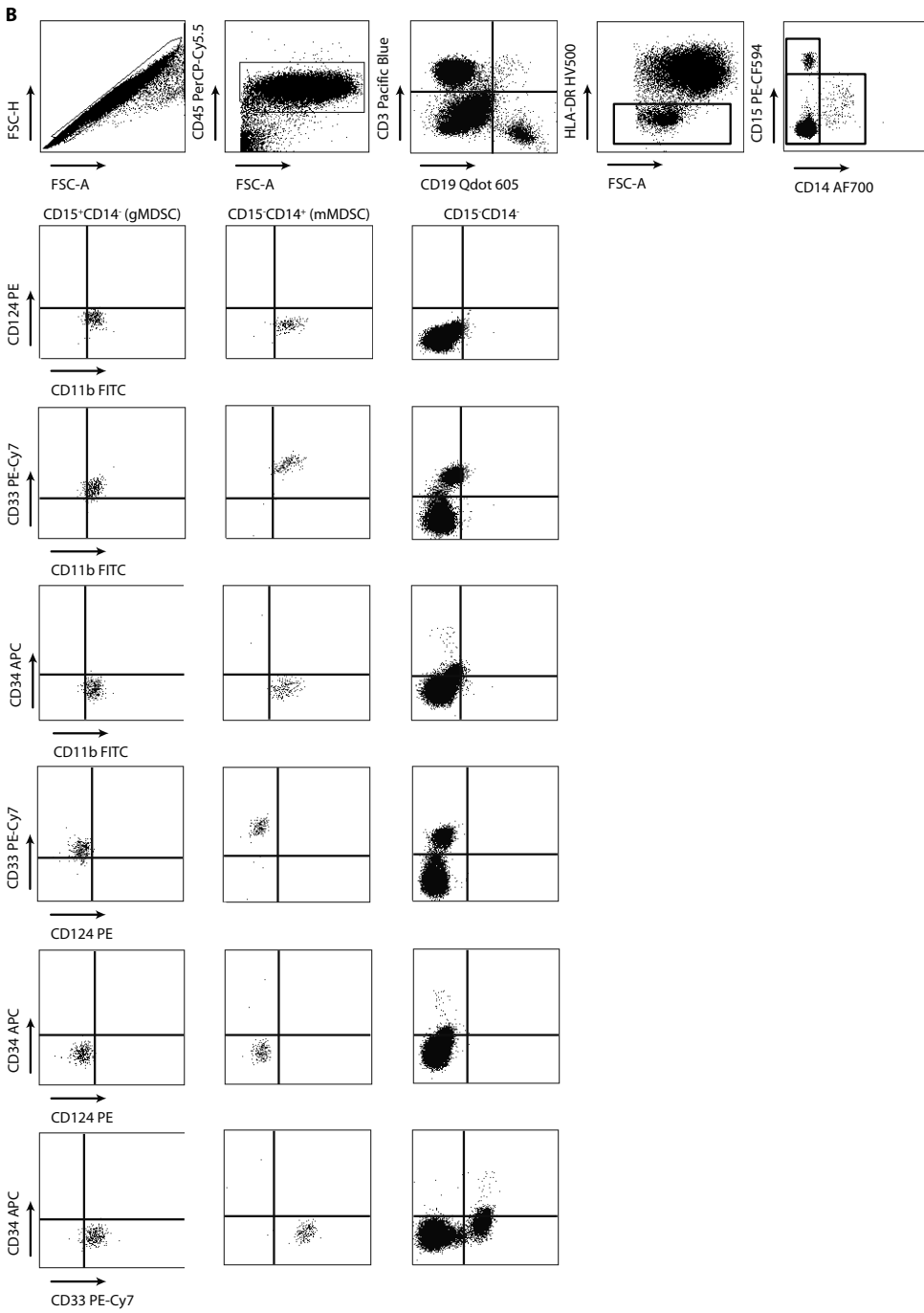

an individual patient. An example of the gating strategy is shown for these three sets of antibodies. (**A**) In the macrophage-like set, first the single cells were gated, then the $CD45^+$ cells followed by the selection of non T and non B cells ($CD3^-$ / $CD19^-$). Then, the HLA-DR^+ / $CD1a^-$ cells were selected. Next, this myeloid cell population is plotted for the expression of CD14 and CD11b revealing 5 subpopulations. Each of these subpopulations were

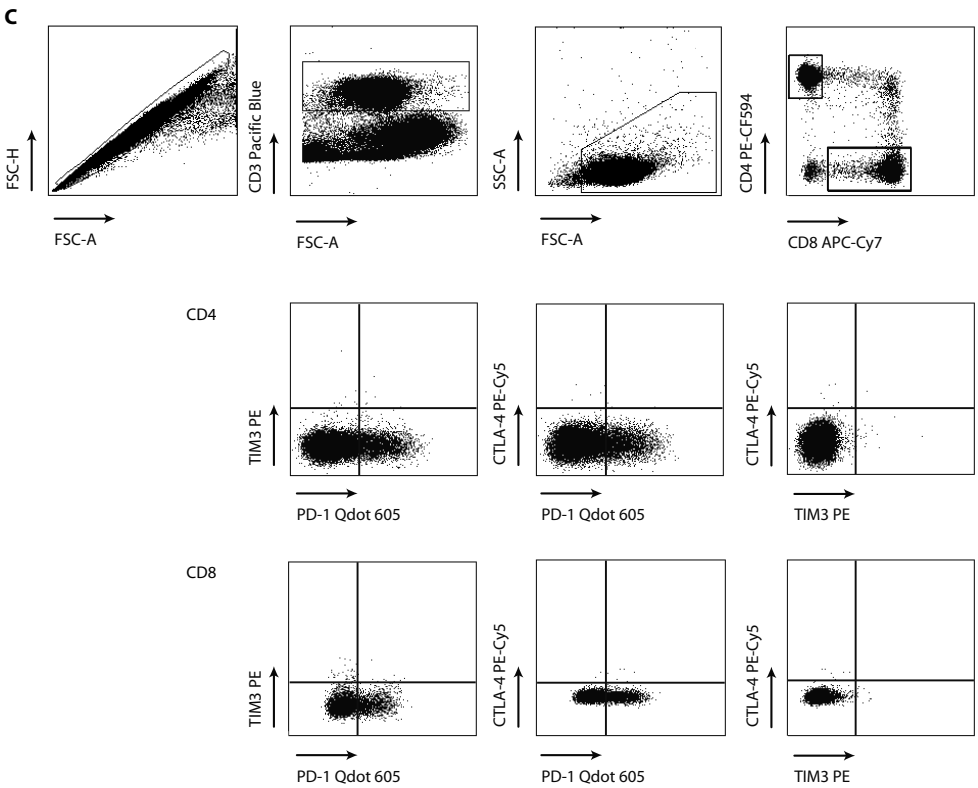

then analyzed for the expression of CD11c, CD16 and CD206, CD163. (**B**) In the myeloid-derived suppressor cell (MDSC) set the same strategy as in the macrophage panel is used for the first three plots. Then, the HLA-DR-/low within the myeloid cells ($CD3^-$ / $CD19^-$) were selected and the expression of CD14 (for myeloid MDSC; mMDSC) and CD15 (for granulocytic MDSC; gMDSC) plotted. Both subsets of MDSC as well as the double negative cells ($CD14^-$ / $CD15^-$) were analyzed for the expression of the other markers CD11b, CD33, CD34 and CD124. (**C**) In the inhibitory receptors set the $CD3^+$ cells were selected from the single cells, followed by the live gate. Then, the CD4 was plotted versus CD8 and within each of these two T-cell populations the expression of TIM-3, PD-1 and CTLA-4 was determined.

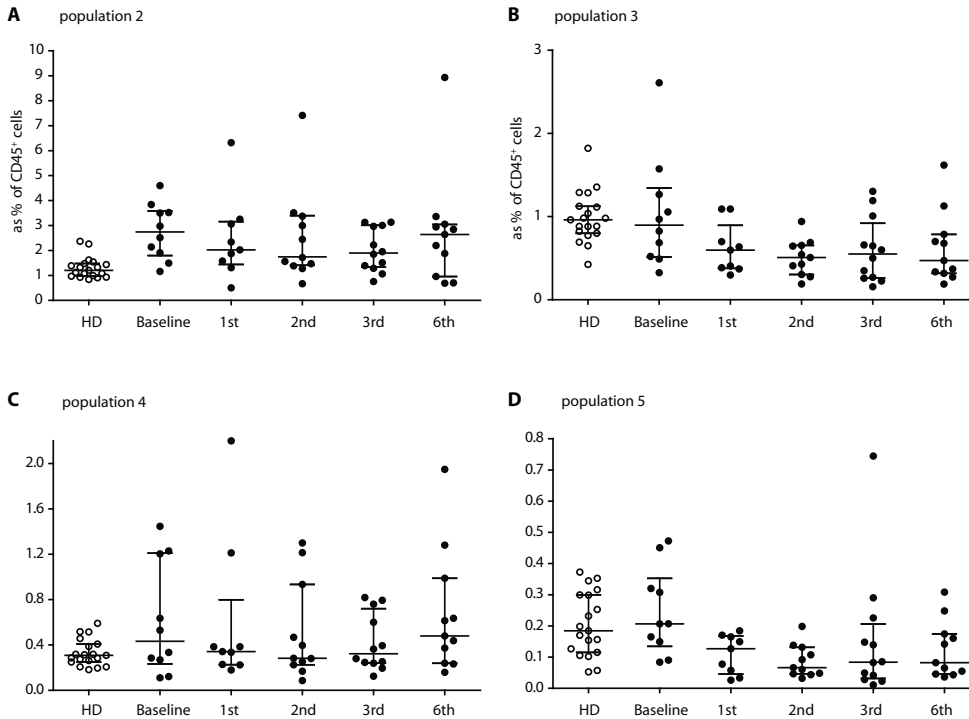

Figure S8. The effect of CarboTaxol on different populations of CD11b and/or CD14 positive myeloid cells. The phenotypic analysis of the blood samples of the cervical cancer patients using the macrophage antibody set and using the gating strategy as shown in fig. S7A, for the 5 different populations which could be defined within the $CD45^+CD3^-CD19^-CD1a^-HLA\text{-}DR^+$ subpopulation of cells due to differential expression of the markers CD14 and CD11b. These subsets of cells were followed over time in all 12 vaccinated patients of cohort 2 and are plotted as median plus interquartile range. (**A**) population 2, harboring intermediate expression of both CD14 and CD11b. Column 1 *vs* 2 (p=0.005), 3 (p=0.03), 4 (p=0.01) and 6 (p=0.004). (**B**) population 3, lacking the expression of both markers. Column 1 *vs* 3 to 6 (p<0.0001). Column 2 *vs* 3 and 6 (p=0.04), 4 (p=0.004). (**C**) population 4, with intermediate CD11b expression and no CD14. Column 1 *vs* 6 (p=0.03). (**D**) population 5, having intermediate CD14 expression and lack of CD11b. Column 1 *vs* 4 (p=0.008). Column 2 *vs* 3 and 6 (p=0.02), and 4 (p=0.002). Data (shown as median plus interquartile range) is analyzed by repeated measures model.

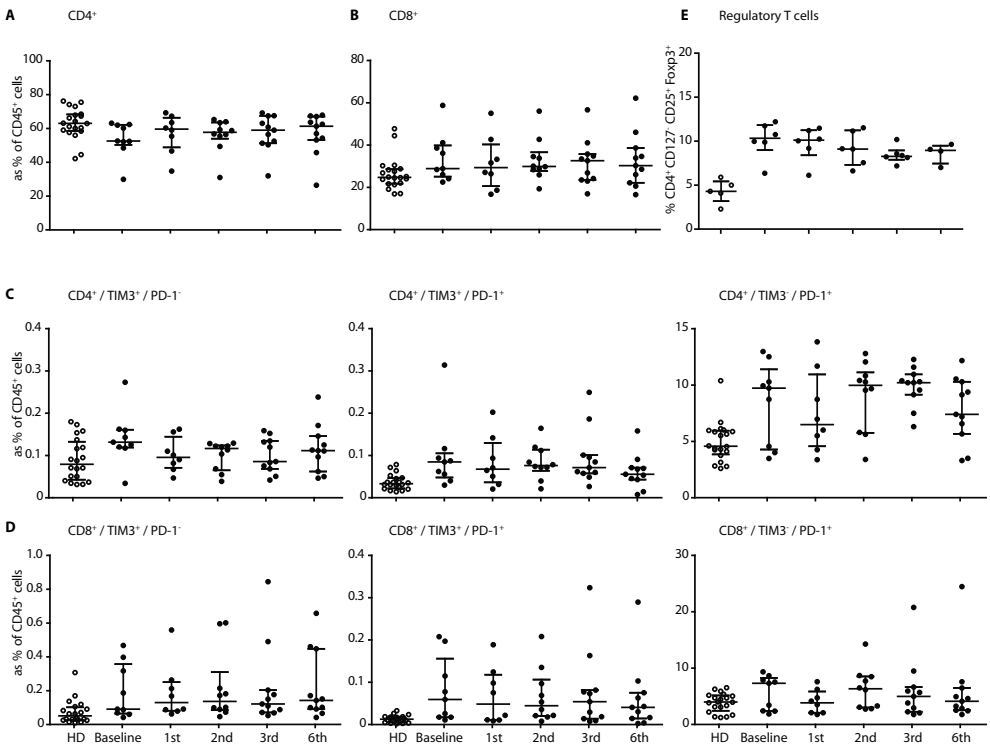

Figure S9. A phenotypic analysis of circulating T cells during CarboTaxol therapy.

The T cells in the blood samples of the cervical cancer patients of cohort 2 as well as from healthy donors (HD) were stained for multiple markers indicative for inhibitory receptors. The frequency is depicted as percentage of the CD45+ cells. (**A**) $CD4^+$ T cells (Column 1 *vs* 2 (p=0.009)). (**B**) $CD8^+$ T cells. (**C**) The frequency within the $CD4^+$ T cells calculated as percentage of $CD45^+$ cells that express TIM3 (left; column 1 *vs* 2 (p=0.01); column 2 *vs* 4 (p=0.002), 5 and 6 (p=0.01)), both TIM3 and PD-1 (middle; column 1 *vs* 2 (p=0.007), 3 (p=0.01), 4 (p=0.04) and 5 (p=0.004)) or PD-1 (right; column 1 *vs* 2 (p=0.0008), 3 (p=0.001), 4 (p=0.0001), 5 (p<0.0001) and 6 (p=0.002)). (**D**) The frequency within the $CD8^+$ T cells calculated as percentage of $CD45^+$ cells that express TIM3 (left; column 1 *vs* 2 (p=0.01), 3 (p=0.004), 4 (p=0.02), 5 (p=0.004) and 6 (p=0.009)), both TIM3 and PD-1 (middle; column 1 *vs* 2 (p=0.008), 3 (p=0.01), 5 (p=0.03)) or PD-1 (right; column 1 *vs* 2 (p=0.04)). (**E**) Measurement of regulatory T cells within the $CD3^+CD8^-CD4^+$ population by expression of $CD25^+$, $CD127^-$ and $FoxP3^+$ (Column 1 *vs* 2 and 3 (p<0.0001), 4 (p=0.001) and 5 (p=0.002); column 2 *vs* 4 (p=0.007) and 5 (p=0.005). Data (shown as median plus interquartile range) is analyzed by repeated measures model.

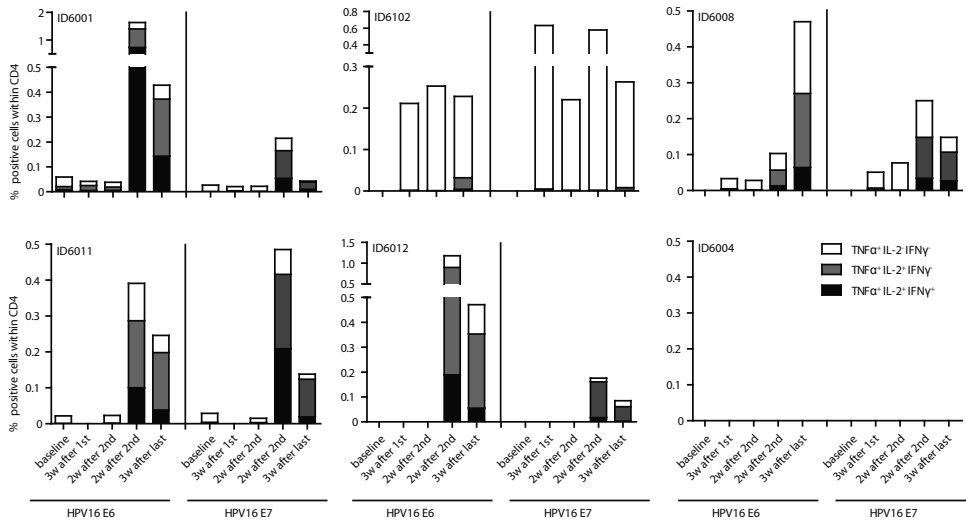

Figure S10. HPV16-SLP vaccination induces polyfunctional T cells.
Of 6 patients in the second cohort an in depth analysis by intracellular cytokine staining could be performed to determine the cytokine production specifically upon recognition of HPV16 E6 and/or E7 peptides. In the stacked bars the frequency of $CD4^+$ T cells producing only TNFα ($TNFα^+$ $IL\text{-}2^-$ $IFNγ^-$; white bars), both TNFα and IL-2 ($TNFα^+$ $IL\text{-}2^+$ $IFNγ^-$; grey bars) and the triple cytokine producers (($TNFα^+$ $IL\text{-}2^+$ $IFNγ^+$; black bars) are shown for the two viral oncoproteins in the indicated blood samples.

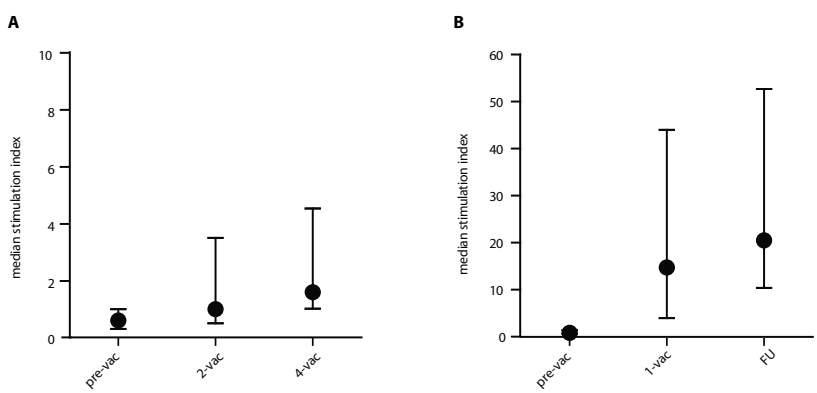

Figure S11. A comparison of the HPV16-specific T-cell response in patients vaccinated during or after chemotherapy.
The median stimulation index (plus interquartile range) of the 6 tested peptide pools per patient was calculated for all patients per indicated time point and depicted for the (**A**) recurrent cervical cancer patients in the previously conducted clinical trial (*15*), in which the patients received HPV16-SLP vaccination at least one month after they had undergo chemotherapy and (**B**) advanced cervical cancer patients who were vaccinated during the chemotherapy as described in the current trial. The blood samples were taken prior to vaccination (pre-vac), after 1 (1-vac), 2 (2-vac) or 4 (4-vac) vaccination as indicated. FU, follow-up blood sample taken after the last cycle of chemotherapy. In both graphs the pre-vaccinated median stimulation index is significantly different from the two post-vaccinated responses ($p < 0.0001$). Data is analyzed by paired T-test.

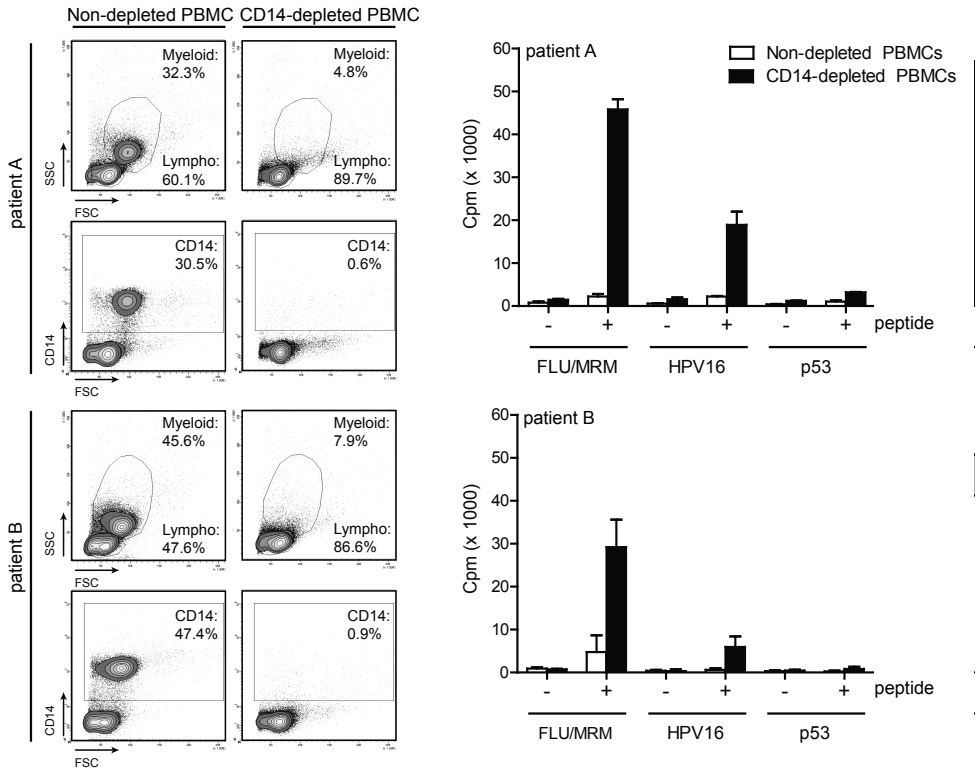

Figure S12. Myeloid cell depletion improves the response of PBMC to stimulation in vitro.
The CD14$^+$ myeloid cells were depleted in the pre-chemotherapy PBMC sample of two advanced cervical cancer patients via magnetic cell sorting. The depleted and non-depleted PBMC were stimulated with autologous monocytes, which were pulsed either with a mix of recall antigens (FLU and MRM), a pool of HPV16 E6 and E7 SLP or a pool of p53 SLP, for 11 days where after the bulk culture was tested in a 3-days proliferation assay. On the left the forward (FSC) and side (SSC) scatter plots are shown for both the non-depleted and depleted PBMC. The percentages indicate the frequencies of lymphoid and myeloid cells. In the FSC and CD14 plots the CD14$^+$ cell frequencies in PBMC before and after the CD14 depletion are shown. On the right, the graphs display the antigen-specific proliferation (in counts per minute, cpm, as mean of triplicate wells plus standard deviation) for the three different bulk cultures after stimulation with non-pulsed (peptide -) or antigen-pulsed (peptide +) autologous monocytes.

Table S1A. Patient characteristics

	Age			Primary Tumor		Advanced / Recurrent / Metastatic Disease					
ID	D	R	I	FIGO	Treatment	Disease	Interval P-R (months)	Prior treatments	No. of cycles CarboTaxol	Dose Carboplatin	Dose aclitaxel
1	51	52	52	IIB	CHRT	recurrent	6	none	3	normal	normal
2	60	60	60	IV	CHRT	advanced	n.a.	n.a.	6	reduced	reduced
3	32	38	39	IB2	SUR + RT	metastatic	73	CH+RT+HT (cisplatin)	6	normal	normal
4	45	49	50	IB1	SUR + RT	metastatic+ recurrent	47	RT	6	normal	normal
5	55	56	56	IIA	SUR + RT	metastatic	18	none	6	normal	normal
6	36	36	36	IIIB	CHRT	metastatic	8	none	5	normal	normal
6001	50	50	50	IV	CH	advanced	n.a.	n.a.	6	normal	normal
6002	54	56	56	IB1	SUR + RT	metastatic	24	CT + RT (cisplatin)	1	normal	normal
6102	47	48	48	IB1	SUR + CHRT	recurrent	14	none	6	normal	normal
6003	42	45	45	IB1	SUR + CHRT	metastatic	35	none	6	normal	normal
6004	32	33	33	IIB	RT + BT + HT	recurrent	5	none	3	normal	normal
6005	35	37	37	IB1	SUR	recurrent	22	none	6	normal	normal
6006	34	35	36	IIB	CHRT + HT	recurrent	22	alternative	6	reduced	reduced
6007	49	55	55	IB1	SUR + CHRT	recurrent	64	none	6	normal	normal
6008	70	71	71	IIIB	RT + BT + HT	metastatic	21	none	6	reduced	reduced
6009	29	34	34	IA1	SUR	metastatic	56	none	6	normal	normal
6010	33	36	37	IIB	SUR + CHRT	metastatic	37	CT + RT (cisplatin)	6	normal	normal
6011	28	29	31	IB1	SUR	metastatic+ recurrent	16	RT	6	normal	normal
6012	58	58	58	IV	CH	advanced	n.a.	n.a.	6	normal	normal

Table S1B. Patient characteristics

		Vaccination		
ID	**Tumor HPV type**	**Interval CH-vacc (days)**	**Interval vacc-CH (days)**	**No. of vacc**
1	16	n.a.	n.a.	0
2	16	n.a.	n.a.	0
3	18	n.a.	n.a.	0
4	16	n.a.	n.a.	0
5	16	n.a.	n.a.	0
6	16	n.a.	n.a.	0
6001	16	17	6	1
6002	16	n.a.	n.a.	0
6102	16	18	3	1
6003	16	13	8	1
6004	-#	15	6	1
6005	16	15	6	1
6006	-	14	15	1
6007	-	15	6	1
6008	-	17*	15$	1
6009	16	15	6	1
6010	16	13	8	1
6011	16	15	6	1
6012	-	17	4	1

Age at diagnosis (D) of cervical cancer. Age at first recurrence (R), metastatic disease or advanced stage of disease. Age at which the patient was included (I) in the trial, this equals the age at start of chemotherapy CarboTaxol. FIGO: International Federation of Gynecology and Obstetrics representing stage of cancer at diagnosis; CHRT: chemoradiation; SUR: surgery; RT: radiotherapy; BT: brachytherapy; HT: hyperthermia, CH: chemotherapy. Interval P-R: interval between primary tumor and (first) recurrence or metastatic disease (in months). n.a.: not applicable. Prior treatments: other treatment for recurrent, metastatic or advanced disease, different than the primary treatment and different than CarboTaxol. Interval CH-vacc, interval between the starting date of the 2nd cycle of CarboTaxol and the date of vaccination with HPV16-SLP. Interval vacc-CH, interval between the date of vaccination and the date of the 3rd cycle (or 4th in case of patient ID6008 $) of chemotherapy with CarboTaxol.
* For patient ID6008, vaccination took place 17 days after the 3rd cycle of chemotherapy with CarboTaxol (vaccination was postponed due to infection). # HPV16 negative, but not tested for other high-risk HPV types.

Table S2. Adverse events systemically and at vaccination site

Systemically	< 24h	> 24h; < 3wks	Vaccine related	Remark
Fever	1		definite	
Fever		2	possible	
Myalgia		1	possible	
Nausea		1	possible	
Vomiting		1	possible	
Painfull extremities		1	probable	
Stitch abcess		1	possible	1 wk after vaccination
Nefrodrain infection		1	possible	2 wks after vaccination

	Time after vaccination					
Locally (Injection sites)	**15 min**	**1 hour**	**4 hours**	**3 weeks**	**>6 weeks***	**Total**
Swelling						
0	2 (17%)	0 (0%)	1 (8%)	3 (25%)	3 (27%)	0 (0%)
< 5	9 (75%)	9 (75%)	9 (75%)	4 (33%)	7 (64%)	5 (42%)
5-10	1 (8%)	3 (25%)	2 (17%)	5 (42%)	1 (9%)	7 (58%)
>10	0 (0%)	0 (0%)	0 (0%)	0 (0%)	0(0%)	0 (0%)
Erythema						
none	3 (25%)	2 (17%)	4 (33%)	6 (50%)	7 (64%)	1 (8%)
mild	9 (75%)	10 (83%)	7 (58%)	4 (33%)	3 (27%)	8 (67%)
moderate	0 (0%)	0 (0%)	1 (8%)	2 (17%)	0 (0%)	2 (17%)
severe	0 (0%)	0 (0%)	0 (0%)	0 (0%)	1 (9%)	1 (8%)
Temperature						
none	2 (17%)	1 (8%)	4 (33%)	4 (33%)	10 (91%)	0 (0%)
mild	10 (83%)	11 (93%)	8 (67%)	7 (58%)	1 (9%)	11 (92%)
moderate	0 (0%)	0 (0%)	0 (0%)	1 (8%)	0 (0%)	1 (8%)
severe	0 (0%)	0 (0%)	0 (0%)	0 (0%)	0 (0%)	0 (0%)
Pain						
none	9 (75%)	10 (83%)	9 (75%)	6 (50%)	7 (64%)	6 (50%)
mild	1 (8%)	2 (17%)	3 (25%)	5 (42%)	4 (36%)	3 (25%)
moderate	2 (17%)	0 (0%)	0 (0%)	0 (0%)	0 (0%)	2 (17%)
severe	0 (0%)	0 (0%)	0 (0%)	1 (8%)	0 (0%)	1 (8%)
Itch						
none	12 (100%)	12 (100%)	10 (83%)	7 (58%)	11 (100%)	6 (50%)
mild	0 (0%)	0 (0%)	2 (17%)	5 (42%)	0 (0%)	6 (50%)
moderate	0 (0%)	0 (0%)	0 (0%)	0 (0%)	0 (0%)	0 (0%)
severe	0 (0%)	0 (0%)	0 (0%)	0 (0%)	0 (0%)	0 (0%)
Ulceration	0 (0%)	0 (0%)	0 (0%)	0 (0%)	1 (9%)	1 (8%)

Table S2. (continued)

CTCEA	Administered SLP: E6	E6/E7
grade 1	5 (42%)	6 (50%)
grade 2	6 (50%)	6 (50%)
grade 3	1 (8%)	0 (0%)

Systemic adverse events (AE) observed in the 12 patients in cohort 2, which might be vaccine related and defined as definite, probably or possible. Local adverse event (AE at injection site) of all 12 patients in cohort 2 who received the single HPV16-SLP vaccination. Shown are the number (N) and the percentage (%) of a total of 12 patients. Scoring of injection site AEs at different indicated visits: 15 minutes, 1 and 4 hours as well as 3 and at regular visits >6 weeks after vaccination. * Long-term follow-up (>6 weeks) could not be established for one patient as she deceased (N=11 at > 6 weeks). Total reflects the maximal injection site reaction for each patient as determined for both the E6 and E6/E7 vaccination sites.